ADHESION AND DEFORMATION DURING THERMOCOMPRESSION BONDING OF VERTICALLY ALIGNED CARBON NANOTUBE TURFS TO METALLIZED SUBSTRATES

By

RYAN DAVID JOHNSON

A thesis submitted in the partial fulfillment of
the requirements for the degree of

MASTER OF SCIENCE IN MATERIALS SCIENCE AND ENGINEERING

WASHINGTON STATE UNIVERSITY
Department of Mechanical and Materials Engineering

December 2008

To the faculty of Washington State University:

The members of the Committee appointed to examine the thesis of RYAN DAVID JOHNSON find it satisfactory and recommend that it be accepted.

_____
Chair

_____

_____

_____

ACKNOWLEDGMENTS

There were many faculty and staff who assisted me with my research and whose help I would like to acknowledge. Thank you to the members of my committee, Dr. Cecilia Richards, Dr. Robert Richards, and Dr. Mohamed Osman, for their help, advice, and willingness to provide their time when requested. Thank you to Devon McClain, Josh Green, and Dr. Jun Jiao at Portland State University for their effort in growing my samples, and in turn trusting me with my assistance in the construction of their samples. Thank you to my lab mates: John Youngsman, Ali Zbib, Leland Weiss, Jeong Hyun-Cho, Hamzeh Bardaweel, Amer Hamdan, John Yeager, Molly Kennedy, and many others, for their willingness to take time out of their busy schedules to assist me. Thank you to Joshah Jennings for his assistance and troubleshooting with my cleanroom processes. Thanks go also to Bob Ames, Jan Danforth and Gayle Landeen at the MME office for tolerating my frequent interruptions and requests.

The biggest thank you goes to my advisor, Dr. David Bahr, for providing me with the opportunity to conduct my graduate work at Washington State University, It was a great honor to work for him these last couple of years, and I will always appreciate the support and advice that he has provided for me. I appreciate the obvious interest and passion that he has for the sciences and for the success of his students, which in turn helped motivate me to provide the best work that I could.

I would finally like to acknowledge the financial support of the National Science Foundation under the NIRT program under grant number CTS-0404370.

ADHESION AND DEFORMATION DURING THERMOCOMPRESSION BONDING OF VERTICALLY ALIGNED CARBON NANOTUBE TURFS TO METALLIZED SUBSTRATES

ABSTRACT

by Ryan David Johnson, M.S.
Washington State University
December 2008

Chair: David F. Bahr

A process to mechanically transfer vertically aligned carbon nanotube (VACNT) turfs using thermocompression bonding has been developed for the use of VACNTs as thermal switches in MEMS devices. Mechanical transfer is accomplished by contacting a VACNT turf sputtered with 300 nm gold into a surface similarly coated in 300 nm of gold. A stress equal to the buckling stress of the turf is applied at 150 °C for a minimum of two hours. The VACNT turf transfers to the new surface upon separation.

There are many issues to overcome before VACNT turfs can be implemented as a thermal switch. The greatest hurdle is a high contact resistance between a CNT and its contacting surface including contact resistance and Van der Waals interactions. VACNTs are grown using chemical vapor deposition (CVD), a process conducted at 700-800 °C, which is too high for VACNTs to be grown directly on MEMS devices. VACNT turfs also adhere readily to many surfaces due to local Van der Waals interactions,

requiring control of the adhesive properties for VACNT turfs to be used as thermal switches.

The average separation stress during mechanical transfer has been shown to be 0.42 MPa, and the strength of the new gold bond has been shown to be 0.55 MPa. Electrical measurements across a transferred VACNT turf has shown a conductivity independent of the imposed strain, up to strains in excess of 200%. Mechanical transfer has also been shown to be possible for arrays of VACNT turfs, as well as patterned transfer of segments off of a large VACNT turf.

TABLE OF CONTENTS

LIST OF TABLES

LIST OF FIGURES

DEDICATION

To my family for teaching me drive and ambition and encouraging me to get an education and challenge myself,

To my parents, David and Lynda, for their emotional and financial support across many years of college education,

To my siblings, Stephanie and Erik, who have my eternal love and admiration,

To my grandparents, aunts, uncles, cousins and friends,

I dedicate this work.

CHAPTER ONE

1 Introduction

1.1 Motivation for Research

Effective thermal switch and thermal interface materials are crucial in the successful operation of MEMS (Micro Electronic Mechanical System) or microelectronic devices. The MEMS micro-engine, for example, produced at Washington State University, uses a thermal switch which allows for the production of electricity using waste heat.[1,2]

Carbon nanotubes have potential for use in heat transfer applications, due to a high thermal conductivity, low heat capacity, and unique mechanical properties. In order for carbon nanotubes to be successfully applied in either case, the adhesive properties of the CNTs must be controlled. Also, contact resistance of CNTs[3] has been found to be a primary factor that limits the effectiveness of CNTs in electrical and thermal applications. The contact resistance needs to be addressed in order for CNTs to be useful. Vertically aligned carbon nanotube (VACNT) turfs have the potential to work as a thermal switch[4] or in a thermal interface.[5]

1.2 Properties of Carbon Nanotubes

Carbon nanotubes (CNTs) have been the center of enormous research attention since their discovery in 1991. Researchers quickly realized that CNTs, single-sheets of graphite rolled into a tube, have potential application in a wide variety of fields, due to

their unique mechanical, electrical, and thermal properties. Improvement in processing techniques has also resulted in more effective applications of CNTs.

The discovery of carbon nanotubes is credited to Sumio Iijima.[6] He discovered the carbon nanotubes in the soot of the arc discharge of a carbon anode, and are shown in electron micrographs in Figure 1.1. The wide potential application of carbon nanotubes was quickly realized, and there continues to be immense interest in finding new and novel applications for the relatively new material, due to the properties of carbon nanotubes, and the continuing improvement of processing techniques.

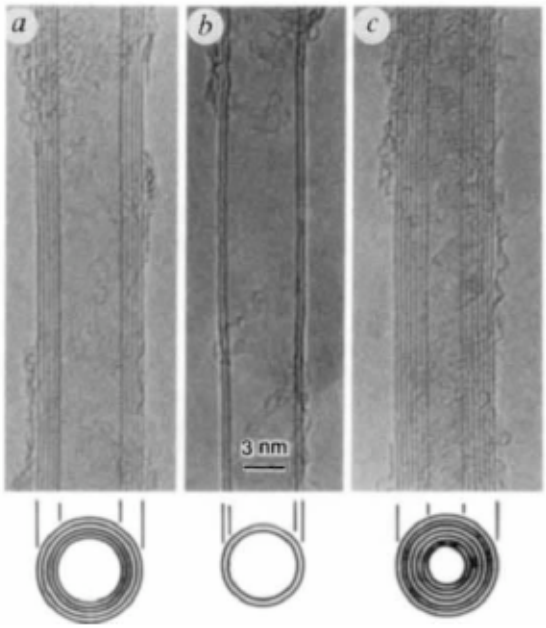

Figure 1.1 - An electron micrograph of individual CNTs. From Iijima.[6]

Carbon nanotubes are sheets of graphene that are rolled into a tube.[7] There are two forms: single-walled carbon nanotubes (SWCNTs), and multi-walled carbon nanotubes (MWCNTs). SWCNTs and MWCNTs can be formed depending on the

process and parameters used during the process. Distinctions between these two forms have to be made, due to the vast difference in properties.

SWCNTs can be described by a chiral vector $\vec{C}$. Given that n and m are integers and $\vec{a}_1$ and $\vec{a}_2$ are unit cell vectors of the lattice formed by unrolling the SWCNT back into a graphene sheet, $\vec{C}$ is defined as

$$\vec{C} = n\vec{a}_1 + m\vec{a}_2$$

This chiral vector determines properties of the nanotube, including whether it is "zig-zag", "armchair", or "chiral". A chiral SWCNT is any SWCNT that is not zig-zag or armchair. The chiral vector has a considerable effect on properties, including determining whether or not the nanotube is metallic or semiconducting, and the mechanical properties that it has.[8]

Figure 1.2 - A visualization of the chiral vector on a sheet of graphene. From Paradise.[9]

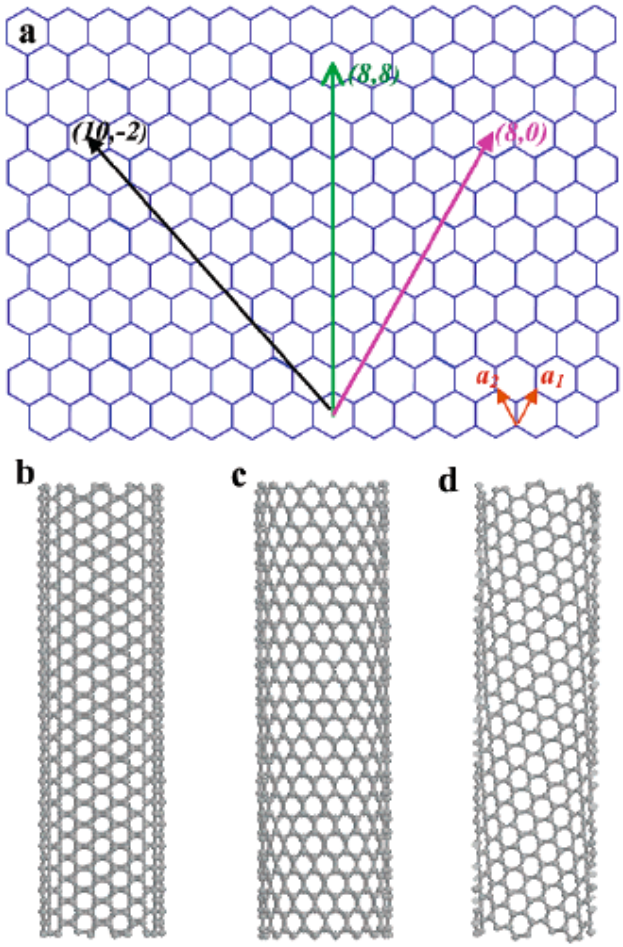

Figure 1.3 - The structure and properties of a SWCNT can vary depending on how a graphene sheet is folded along the chiral vector. (b) armchair CNT (8,8) (c) zigzag CNT (8,0) (d) chiral CNT (10,-2). From Dai.[10]

Multi-walled carbon nanotubes (MWCNTs) have vastly different properties than SWCNTs, and cannot be described simply by the chiral vector. The most commonly observed type of MWCNT is a coaxial type tube, where individual graphene sheets are wrapped about graphene sheets already formed into a tube. There are also MWCNTs that follow a "scroll" model, where a single graphene sheet is rolled into a nanotube like a

scroll of paper. Finally, larger MWCNTs can sometimes demonstrate a coaxial polygonized structure. These three models are shown in Figure 1.4.

(a) **(b)** **(c)**

Figure 1.4 - Three models that describe the structure of MWCNTs. (a) Coaxial, the commonly accepted model. (b) Coaxial polygonized, typical occurs in larger tubes (c) Scroll, not typically observed. From Dresselhaus.[11]

Carbon nanotubes have exceptional mechanical properties. They have been shown to have a modulus of elasticity on the order of 1TPa, and are one of the strongest materials in existence when pulled in a tensile direction.[12] This is due to the strong carbon-carbon bond in the nanotube structure. This strength leads to applications within composite materials.

MWCNTs have a different failure mechanism than SWCNTs when pulled in a tensile direction. In a coaxial structure, for example, individual sheets of the nanotubes are adhered to each other through Van der Waals interactions, which is a much weaker interaction that the C-C bonds in the nanotube structure. As a result, the Van der Waals bonds fail first, and the individual nanotubes slide past each other when they're pulled in a tensile direction. This is referred to as "sword-and-sheath" failure[13], and results in a much lower tensile strength for MWCNTs.

CNTs have a very high thermal conductivity. Also, the strong carbon-carbon bond allows CNTs to handle very high current densities. SWCNTs have been shown to demonstrate ballistic behavior[14], meaning that the mean free path of electrons is effectively greater than the size of the nanotube. Electrons travels essentially unimpeded through the CNT, causing very little heat dissipation, further increasing the allowed current density before failure of the nanotube.

Electron flow can also be controlled through the chirality of the CNT. Armchair CNTs demonstrate metallic behavior, while zig-zag CNTs can demonstrate both semiconducting and metallic behavior, depending on the chiral vector. Chiral CNTs can also be semiconducting or metallic. The semiconducting properties of CNTs give CNTs the ability to be used as transistors.[15]

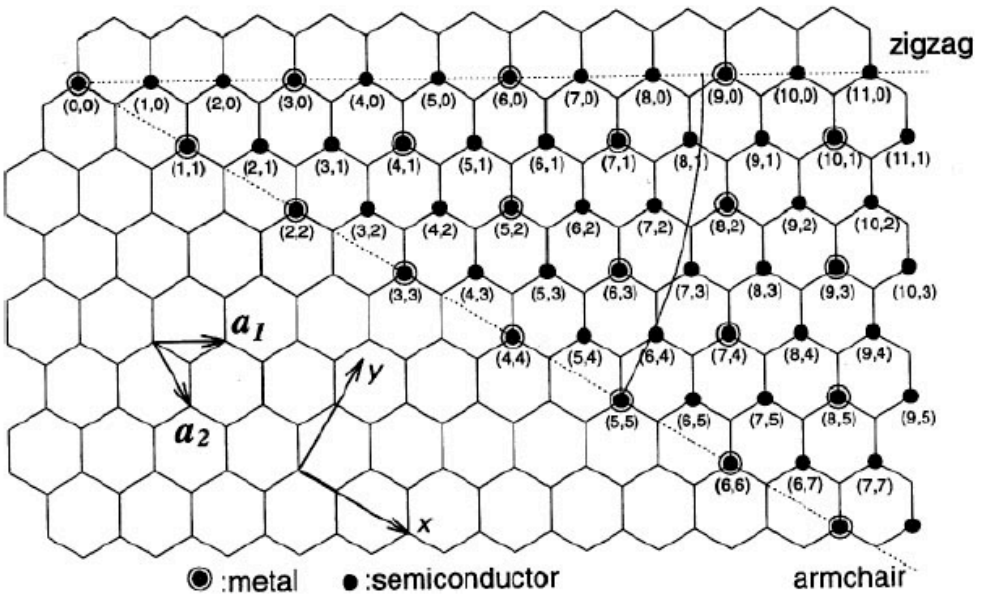

Figure 1.5 - Examples of different chiral vectors and the type of SWCNTs that are produced as a result. From Terrones.[16]

CNTs are theoretically one of the best thermal conductors known. CNTs have been shown to have a thermal conductivity of 3000 W/m*K, and has been reported to be as high as 6600 W/m*K.[17] This very high thermal conductivity means that CNTs have potential application as heat transfer devices. However, contact resistance prevents high theoretical conductivity values from being achieved. Thermal transport in CNTs have been shown to be both phonon and electron controlled.[18] This leads to issues with contact resistance when trying to use CNTs as a thermal switch, considering that in most cases, the CNTs will contact a metallic surface, which is electron transport dominant. This requires a coupling to take place, increasing contact resistance.

A limited understanding of the thermal conductivity of the CNT can be developed through electrical tests of the CNTs, since both have electron flow as part of their transport mechanisms. However, when the temperature of, for example, metallic CNTs is increased, the electrical conductivity decreases due to increased scattering, while the thermal conductivity increases and levels off, as shown by Kim.[19] This makes it difficult to couple electrical and thermal conductivity in this case.

1.3 Applications of Carbon Nanotubes

The unique mechanical, thermal, and electrical properties allow for CNTs to be used in many applications. Potential has been found in MEMS[20] and microelectronics, as thermal switches or permanent thermal channels, with the potential to replace lead-free solder bumps in flip-chip microelectronics. With recent interest in finding methods to store hydrogen, carbon nanotubes have become a candidate for hydrogen storage.[21] CNTs are also useful candidates for use in composites.[22] Their high current density

provides application in field emission devices.[23] High surface energy and Van der Waals interactions lead to application of CNTs to mimic gecko feet[24], and may even be used in the production of a Spiderman suit.[25] Their small diameter and unique interaction properties lead to application as probe tips in scanning probe microscopes.[26]

As processing methods continue to improve, including improvements in purity, controllability of the length, and a decrease in cost, more potential applications of CNTs will be found.

1.4 Carbon nanotube growth methods

There are three primary techniques used in the growth of CNTs. Laser ablation, arc discharge, and chemical vapor deposition (CVD) are all methods that successfully grow CNTs. There are pros and cons to each method, however, including the type, and most importantly to research within this thesis, spatial orientation of CNTs.

Arc discharge was the first method successfully used to produce CNTs. Carbon anodes and cathodes are brought close together, usually about 1mm apart, and then a potential is applied to produce an arc. The anode erodes due to the arcing, and the cathode collects the residue, which contains soot and CNTs. This method benefits from being cheap and relatively easy. However, the process produces low purity, randomly oriented nanotubes.[27] A diagram of the process is shown in Figure 1.6.

Laser ablation allows for the production of very pure nanotubes. A graphite target, inside a heated, inert chamber, is struck with a pulsed laser. Carbon nanotube collect on the inside surface of the chamber. This method produces very pure nanotubes,

but suffers from high expense, and again a random orientation of the nanotubes.[28] A diagram of this process is shown in Figure 1.6.

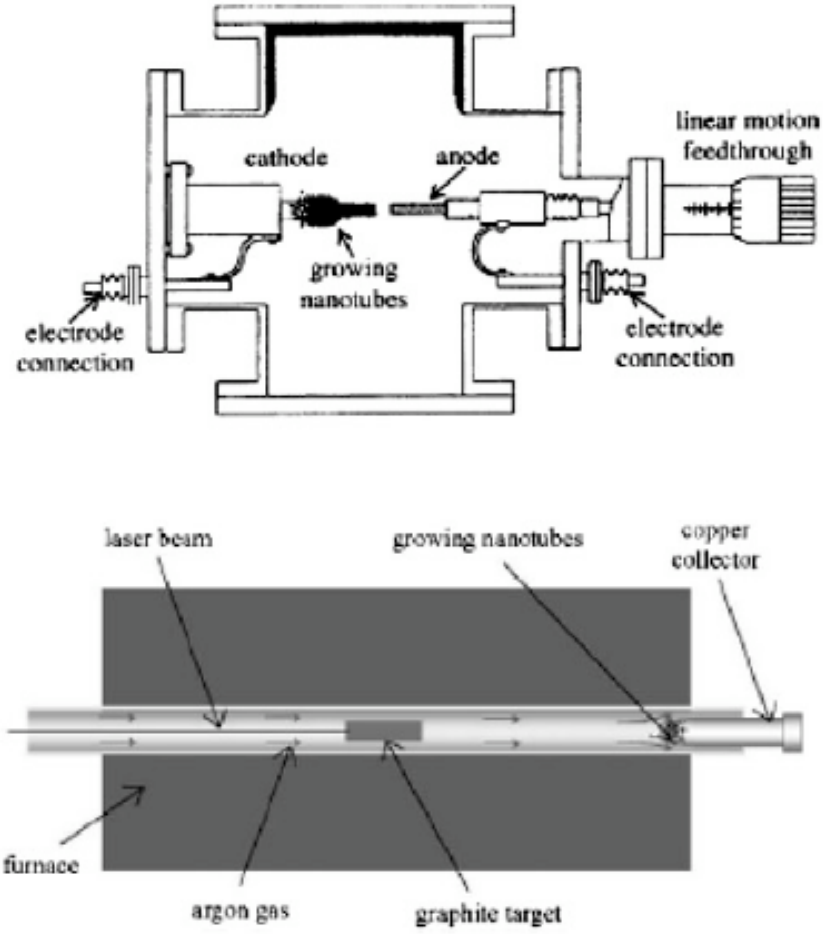

Figure 1.6 - Schematic of arc discharge and laser ablation. From Paradise.[29]

Chemical vapor deposition (CVD), has received a lot of interest recently for a number of reasons. CVD allows for the inexpensive, mass-produced, patterned growth of vertically aligned carbon nanotubes (VACNTs).[30] Unlike arc discharge or laser ablation,

the orientation of carbon nanotubes grown in this method can be controlled. This is a powerful result that opens up new applications in MEMS and microelectronics, including making it a useful processing method for the production of the MEMS micro-engine's thermal switch. Details of the CVD process will be detailed in the next chapter.

1.5 Nanoindentation of VACNT Turfs

CVD produces an entangled, nominally vertical forest of pre-bent, pre-buckled SWCNTs and MWCNTs. It is a fairly hollow structure, with a low packing fraction of ~2%. The structure grows in a nominally vertical direction due to the balance between strain energy and contact energy in the CNTs. This structure has been found to have drastic differences in behavior than individual SWCNTs and MWCNTs.

(a) (b)

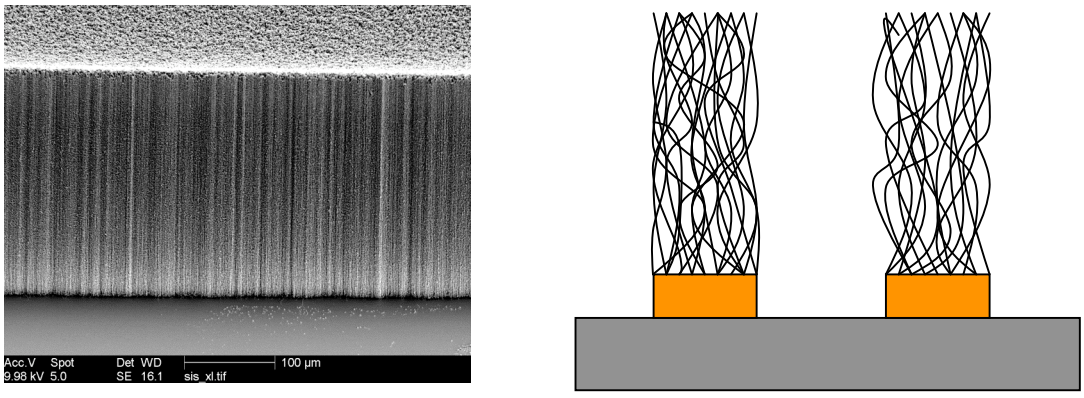

Figure 1.7 - (a) The side of a gold-coated VACNT turf, showing the entangled, nominally vertical structure. (b) A diagram of VACNT turfs growing on sol-gel

To understand the mechanical properties of these structures, a nanoindentation tip was brought into contact with the top of the VACNT turf, as conducted by McCarter.[31]

The nanoindentation procedure showed two very important differences between the properties of VACNT turfs and individual CNTs. First, the effective modulus of the VACNT turfs was shown to be around ~15 MPa, a fraction of the 1 TPa modulus measured for single SWCNTs. This shows that VACNT turfs are very compliant, which is ideal for thermal switches. Nanoindentation data also showed adherence between the nanoindentation tip and the VACNT turf.

Figure 1.8 shows a loading/unloading curve for a nanoindentation tip brought into contact with a VACNT turf. During the unloading portion of the process, which is the right part of the curve, the applied load becomes negative. Some CNTs are adhered to the tip and are pulling against it as it tries to pull away. Contact finally breaks at a certain point, and the tip pulls away. This demonstrates the stickiness of CNTs, due to localized Van der Waals interactions. The adhesion of CNTs is not an ideal property for CNTs to be used in thermal switches, and thus needs to be controlled.

(a) (b)

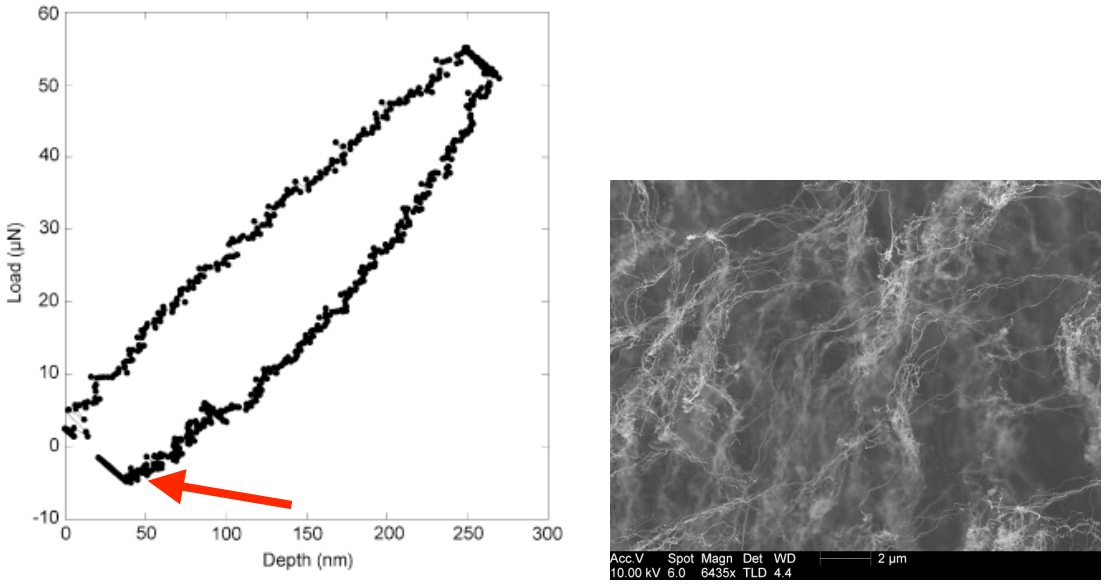

Figure 1.8 - (a) Load/depth curve of a nanoindentation tip brought into the top of a VACNT turf. Red arrow shows adhesion of VACNT turf to the tip. From McCarter.[31] (b) SEM image of the top of a VACNT turf, demonstrating the low packing fraction.

Zbib et al proposed that by sputtering a thin film of gold on top of the VACNT turf, the Van der Waals interactions that cause the CNTs to bond to the nanoindentation tip will be reduced, and bonding will not occur. In determining the desired thickness of the gold film, nanoindentation was conducted on turfs with the thickness of the gold film varying from 150 nm to 500 nm. Although the word "film" is used in describing the gold layer, scanning electron microscopy (SEM) images show that the gold in fact nucleates and deposits on the individual nanotubes rather than uniformly across the entire turf, and encapsulates the individual CNTs. This is shown in Figure 1.9.

(a) (b)

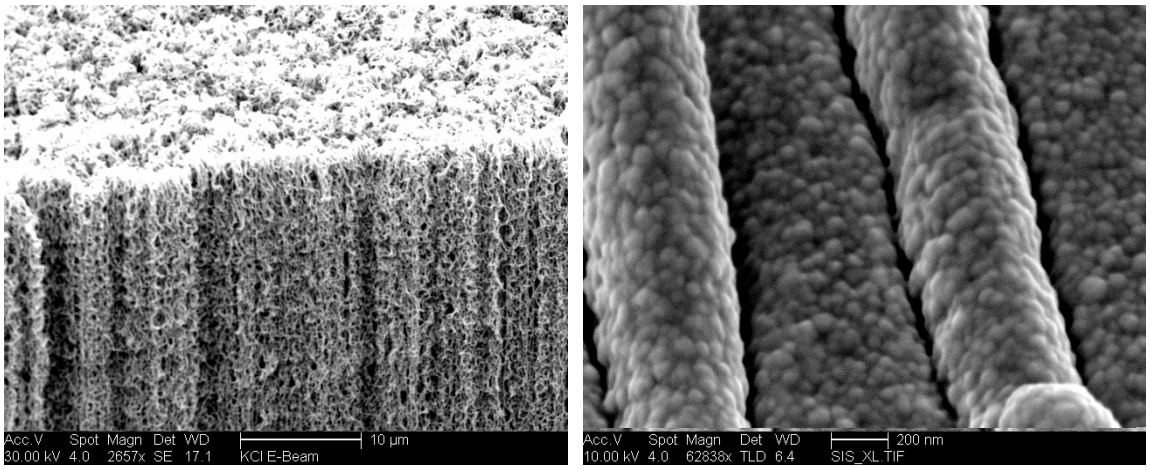

Figure 1.9 - (a) The side and top of a gold coated VACNT turf. The top of the turf is not a uniform film. Rather, the gold encapsulates the individual CNTs. (b) Individual gold coated CNTs, showing individual gold grains.

The nanoindentation tests resulted in two major observations. First, the gold film indeed suppressed Van der Waals interactions. As the nanoindentation tip pulls away from sample, there is no longer a negative dip in the load on the load/depth curve. This means that the CNTs did not pull on the nanoindentation tip, and therefore did not adhere to the tip. A gold film on the top of the VACNT turfs makes the VACNT turfs more ideal for use as a thermal switch.

The nanoindenations of the VACNT turfs with gold films of varying thickness also showed that the effective modulus of the turf is dependant on the thickness of the gold film. Nanoindentation of the VACNT turf with the 500 nm turf resulted in a higher slope during the loading phase of the indentation. This means that the effective modulus of the turf is higher than an uncoated VACNT turf, and the structure is stiffer overall. The VACNT turf with the 300 nm gold layer behaves much differently, and actually had

a lower slope during loading than an uncoated VACNT turf. This is attributed to a result of the reduction of the Van der Waals interactions between the gold coated CNTs within the turf. With little interaction occurring, the individual CNTs are able to slide and rotate past each other more easily as the VACNT turf is compressed. In the 500 nm film, although Van der Waals interactions are reduced, the individual CNTs are in fact less able to slide past each other. An SEM image by McCarter in Figure 1.10 shows the structure of a VACNT turf coated in a 500 nm film. A turf with a 300nm film is also in Figure 1.10, and the differences in the structure are noted. With the 500 nm film, the individual CNTs are coated to a point that they press up against each other more, meaning that they are less able to slide past each other. The 300nm film still leaves some space for the individual CNTs to slide and rotate past each other.

This result suggests that a thinner film of gold on top of a VACNT turf makes VACNTs more ideal for thermal switches by making the structure more compliant and reducing adhesion between the VACNT turf and contacting surfaces. A gold film thickness of 300 nm was decided upon.

(a) (b)

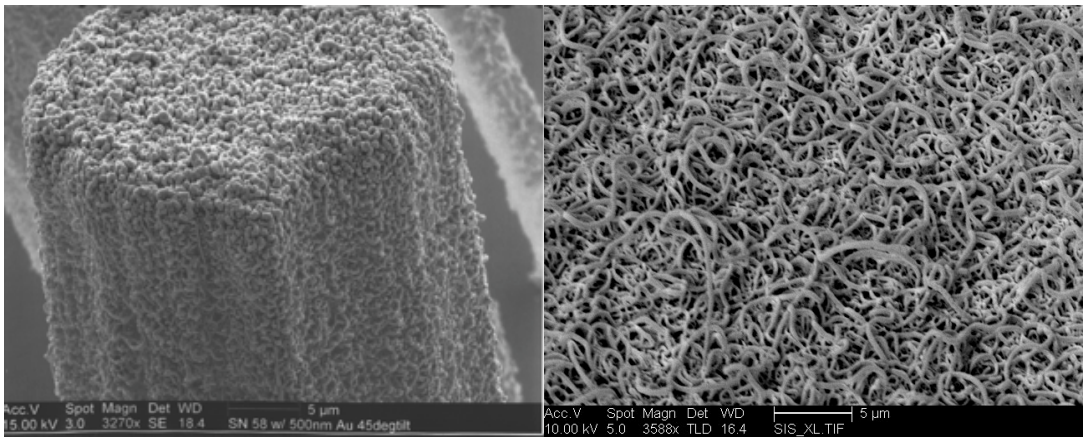

Figure 1.10 - (a) The side and top of a VACNT turf coated with 500 nm of gold. (b) The top of a VACNT turf coated with 300 nm of gold. From McCarter.[32]

1.6 Buckling of VACNT turfs

The nanoindentation tests provide data by using a very small tip on a very large turf. The data shows results of the deformation of a very localized area. In contrast, by using a tip that's around the same size as the top of the VACNT turf, the turf behaves very differently, providing a different result and revealing unique behavior for a VACNT turf in compression.

Figure 1.11 shows the result of compressing a VACNT turf with a large probe tip that is the size of the turf, as shown by Zbib.[33] The structure has gone through permanent plastic deformation and has buckled. The buckling occurs in a very unique way, in that all buckling occurs at the base of the turf. This is attributed to the difference in compliance between the VACNT turf and the silicon base. The buckling has also shown that the turf buckles as a unit, rather than as individual CNTs. The buckling tests have also shown that while there is permanent deformation taking place, much of the structure

springs back to its original state upon unloading, a trait that is very useful in thermal switches.

(a) (b)

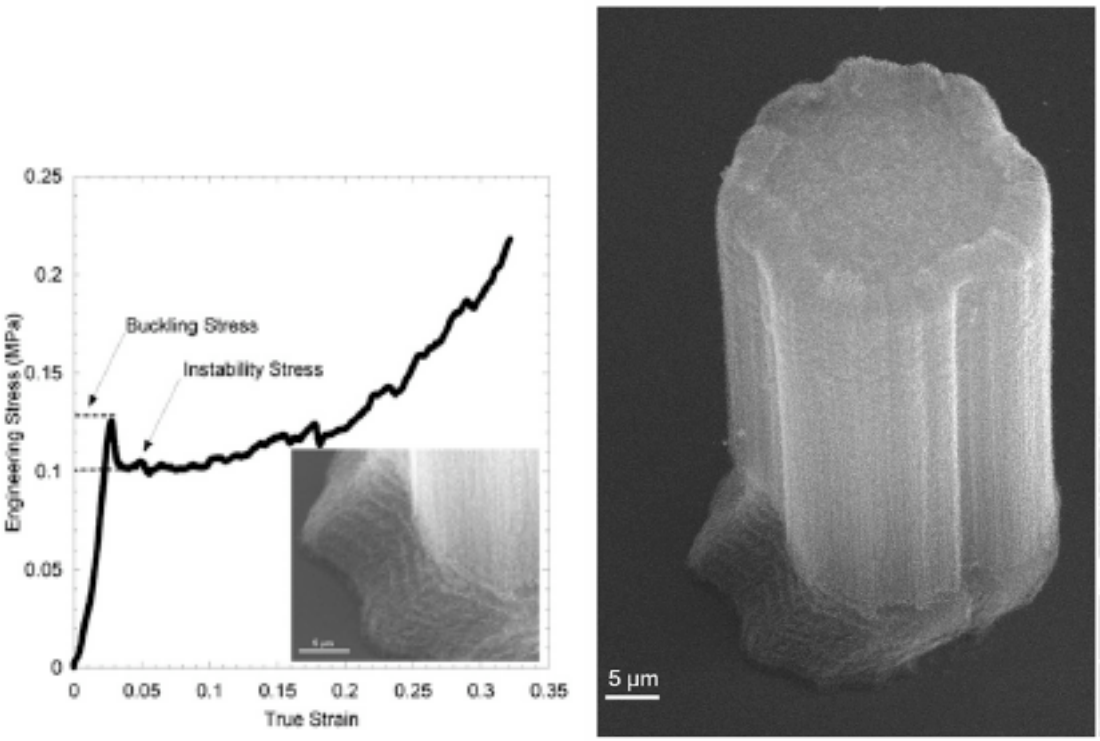

Figure 1.11 - (a) Stress/strain curve, showing the onset of buckling as well as further buckling as stress continues to be applied. (b) A buckled VACNT turf. The distance between individual buckles has been shown to be ~12 μm, independent of turf morphology. From Zbib.[33]

A model was developed by Zbib et al to determine the stress required to buckle a VACNT turf. The result of the model is the equation:

$$\frac{\mu}{\sigma} \approx \frac{1 - h_1 / h}{h_1 / h}$$

Where h is height of the turf, and h_1 is the height of each individual buckle, consistently shown to be approximately 12 μm. σ is the instability stress, while μ is the shear modulus, which is assumed to be half of the elastic modulus. The equation has no mention of the size of the turf, only the height, a result suggesting that the buckling stress of the turf is independent of the lateral size of the turf. Buckling data and a curve fit from the equation are shown in Figure 1.12, showing a decent match to experimental data. This is an important result in this thesis' development of the mechanical transfer method, as will be shown soon.

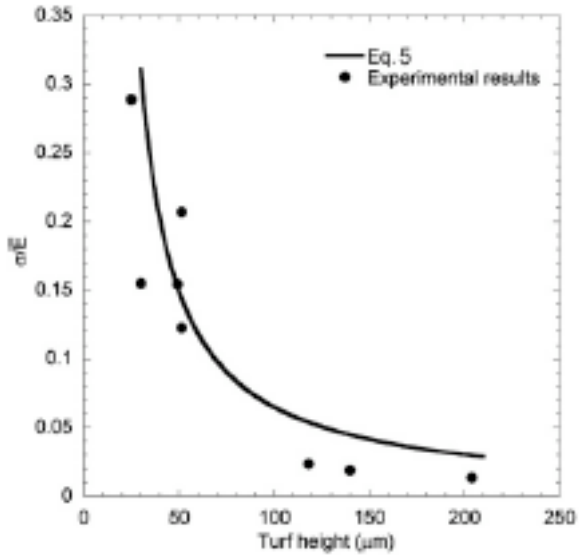

Figure 1.12 - Model demonstrating the effect of the height of the VACNT turf on the stress required to induce buckling. From Zbib.[33]

1.7 Applying VACNTs turfs as a thermal switch

Although VACNT turfs show much promise for use as a thermal switch, there are many issues that must be addressed before they can be feasible.

The primary obstacle in the application of VACNT turfs in a thermal switch is the contact resistance between the carbon nanotube and the contacting surface.[34] Although carbon nanotubes have a very high theoretical thermal conductivity, this value is never reached in reality due to contact resistance. This has been a limiting factor in much of the research being conducted on the thermal and electrical properties of CNTs. In order for VACNT turfs to become feasible thermal channels or switches, the contact resistance needs to be minimized.

A potential reason for thermal contact resistance in CNTs is small contact area and the coupling mechanism that must take place between the phonon transport dominant CNT and the usually metallic, therefore electron transport dominant contact surface. CNTs have a diameter that is usually a fraction of a nanometer across, providing a very small area for coupling to take place. By increasing the contact area, coupling can be increased, and contact resistance can potentially be reduced.

CVD is a very effective method in the growth of VACNT turfs. A major issue is the high growth temperatures, 750 °C, required for CNT growth. Most thermal switches are added to a MEMS device as one of the final steps, and most nearly constructed MEMS devices cannot handle 750 °C temperatures without causing damage to the device. Thus, VACNT turfs cannot be directly grown on the device. A solution to this

issue is to grow the VACNT turfs separately, and then mechanically transfer the VACNT turf to the device within the acceptable temperature limits of the device.

Finally, the adhesive properties of the VACNT turfs need to be controlled in both the permanent channel and switch applications. Due to high surface area and local Van der Waals interactions, CNT turfs will readily bond with many surfaces. This is not ideal in a thermal switch. As shown by Ali et al, sputtering a gold film on the top of the VACNT surface can reduce adherence between VACNTs and the contact surface.

A new method of mechanical transfer of VACNT turfs using thermocompression bonding has been developed, which compensates for all of the issues previously mentioned and takes advantage of the gold film and the properties of the VACNT turf. This process allows for VACNT turfs to be transferred to a MEMS device at 150 °C, and minimizes adherence between the VACNT turf and its contacting surface. This process has the potential to decrease contact resistance by increasing the coupling area from the encapsulation of the CNTs by the sputtering of a gold film.

This thesis will outline the process in growing VACNT samples, as well as the research conducted prior to the development of the thermocompression bonding process. The next chapter will discuss the steps involved in the thermocompression bonding process, and analyze the separation stress and electrical resistance of the VACNT turf during the mechanical transfer to a new substrate. The electrical properties of the completed thermal switch are analyzed, as well as a discussion on the effects of annealing of the gold layers. Finally, the thesis concludes, with an outline of recommendations for future research.

References

[1] Weiss L W, Cho J H, McNeil K E, Richards C D, Bahr D F, Richards R F, "Characterization of a dynamic micro heat engine with integrated thermal switch," J Micromech Microeng 16, S262-S269 (2006)

[2] Cho J H, Weiss L W, Richards C D, Bahr D F, Richards R F, "Power production by a dynamic micro heat engine with an integrated thermal switch," J Micromech Microeng 17, S217-S223 (2007)

[3] Ngo Q, Petranovic D, Krishnan S, Cassell A, Ye Q, Li J, Meyyappan M, Yang C, "Electron Transport Through Metal-Multiwall Carbon Nanotube Interfaces," IEEE T Nanotehnol 3, 311 (2004)

[4] Cho J, Richards C, Bahr D, Jiao J, Richards R, "Evaluation of contacts for a MEMS thermal switch," J Micromech Microeng 18, 105012 (2008)

[5] Xu J, Fisher T S, "Enhancement of thermal interface materials with carbon nanotube arrays," Int J Heat Mass Tran 49, 1658 (2006)

[6] Ijima S, "Helical microtubules of graphitic carbon," Nature 354, 56 (1991)

[7] Thostenson E, Ren Z, Chou T, "Advances in the science and technology of carbon nanotubes and their composites: a review," Compos Sci Technol 61, 1899 (2001)

[8] Belin T, Epron F, "Characterization methods of carbon nanotubes: a review," Mat Sci Eng B 119, 105-118 (2005)

[9] Paradise M, Goswami T, "Carbon nanotubes - Production and industrial applications," Mater Design 28, 1477-1489 (2007)

References

[10] Dai H, "Carbon Nanotubes: Synthesis, Integration, and Properties," Acc Chem Res 35, 1035-1044 (2002)

[11] Dresselhaus M, Dresselhaus G, Eklund P, Saito R, "Carbon nanotubes," Phys World, January (1998)

[12] Treacy M M J, Ebbesen T W, Gibson J M, "Exceptionally high Young's modulus observed for individual carbon nanotubes," Nature 381, 678-680 (1996)

[13] Yu M, Yakobson B I, Ruoff R S, "Controlled Sliding and Pullout of Nested Shells in Individual Multiwalled Carbon Nanotubes," J Phys Chem B 104, 8764-8767 (2000)

[14] White C T, Todorov T N, "Carbon nanotubes as long ballistic conductors," Nature 393, 240 (1998)

[15] Nosho Y, Ohno Y, Kishimoto S, Mizutani T, "Relation between conduction property and work function of contact metal in carbon nanotube field-effect transistors," Nanotechnology 17, 3412-3415 (2006)

[16] Terrones M, "Science and Technology of the Twenty-First Century: Synthesis, Properties and Applications of Carbon Nanotubes," Annu Rev Mater Res 33, 419-501 (2003)

[17] Berber S, Kwon Y K, Tomainek D, "Unusually High Thermal Conductivity of Carbon Nanotubes," Physical Review Letters 84, 4613 (2000)

[18] Dresselhaus M S, Eklund P C, "Phonons in carbon nanotubes," Adv Phys 49, 705-814 (2000)

References

[19] Kim P, Shi L, Majumdar A, McEuen P L, "Thermal Transport Measurements of Individual Multiwalled Nanotubes," Phys Rev Lett 87, 215502 (2001)

[20] Jungen A, Stampfer C, Hoetzel J, Bright V, Hierold C, "Process integration of carbon nanotubes into microelectromechanical systems," Sensors and Actuators A 130 588-594 (2006)

[21] Lee S M, Lee Y H, "Hydrogen storage in single-walled carbon nanotubes," Applied Physics Letters 76, 2877 (2000)

[22] Wang J, Musameh M, "Carbon Nanotube/Teflon Composite Electrochemical Sensors and Biosensors," Anal Chem 75, 2075-2079 (2003)

[23] Fan S, Chapline M G, Franklin N R, Tombler T W, Cassell A M, Dai H, "Self-Oriented Regular Arrays of Carbon Nanotubes and Their Field Emission Properties," Science 283, 512 (1999)

[24] Ge L, Sethi S, Ci L, Ajayan P, Dhinojwala A, "Carbon nanotube-based synthetic gecko tapes," P Natl Acad Sci 104, 10792-10795 (2007)

[25] Pugno N, "Towards a Spiderman suit: large invisible cables and self-cleaning releasable superadhesive materials," J Phys Condens Matter 19, 395001 (2007)

[26] Hafner J H, Cheung C, Oosterkamp T H, Lieber C M, "High-Yield Assembly of Individual Single-Walled Carbon Nanotube Tips for Scanning Probe Microscopies," J Phys Chem B 105, 743 (2001)

[27] Ebbesen T W, Ajayan P M, "Large-scale synthesis of carbon nanotubes," Nature 358, 220 (1992)

References

[28] Maser W K, Munoz E, Benito A M, Martinez M T, de la Fuente G F, Maniette Y, Anglaret E, Sauvajol J L, "Production of high-density single-walled nanotube material by a simple laser-ablation method," Chemical Physics Letters 292, 587 (1998)

[29] Paradise M, Goswami T, "Carbon nanotubes - Production and industrial applications," Materials and Design 28, 1477- 1489 (2007)

[30] Sinnott S B, Andrews R, Qian D, Rao A M, Mao Z, Dickey E C, Derbyshire F, "Model of carbon nanotube growth through chemical vapor deposition," Chem Phys Lett 315, 25-30 (1999)

[31] McCarter C M, Richards R F, Mesarovic S Dj, Richards C D, Bahr D F, McClain D, Jiao J, "Mechanical compliance of photolithographically defined vertically aligned carbon nanotube turf," J Mater Sci 41, 7872-7878 (2006)

[32] McCarter, C "Mechanical Properties of Vertically Aligned Carbon Nanotubes For Use in a Thermal Switch," [Master's thesis]: Washington State University (2006)

[33] Zbib A A, Mesarovic S Dj, Lilleodden E T, McClain D, Jiao J, Bahr D F, "The coordinated buckling of carbon nanotube turfs under uniform compression," Nanotechnology 19, 175704 (2008)

[34] Xu J and Fisher T S, "Enhancement of thermal interface materials with carbon nanotube arrays," Int J Heat Mass Tran 49, 1658-1666 (2006)

Chapter Two

2 Sample preparation and test development

2.1 Introduction

Chemical vapor deposition (CVD) has been shown to be a useful process for the production of CNTs for use in a thermal switch. The type of structure produced by this process, the vertically aligned, entangled structure, is an ideal orientation for heat transfer in MEMS devices. A sol-gel technique is described, which allows for the use of photolithography to carefully pattern the size and configuration of arrays of VACNTs.

Initial research that led up to the development of the thermocompression bonding procedure is outlined in this chapter. Results of probing an uncoated VACNT turf with a tungsten carbide tip is discussed, along with a discussion of different films that were used in the attempts to mechanically transfer VACNT turfs. Finally, the development of the thermocompression bonding process will be discussed, followed by optimization steps of the bonding process.

2.2 Sol-gel Preparation

VACNT turfs are grown using chemical vapor deposition (CVD) on a patterned sol-gel evenly dispersed with ~10nm iron nanoparticles. The sol-gel process provides many advantages. The process is inexpensive and produces a uniform, controllable layer of iron nanoparticles. Just as important is the ability for the sol-gel to be patterned using standard photolithography techniques. This allows for the controlled growth of VACNT

turfs, and allows for the growth of large single turfs or arrays of turfs as small as a few microns across.

The sol-gel is prepared by first mixing tetraethyl orthosilicate (TEOS) and ethyl alcohol, which is stirred for 15 minutes on a hot plate using a stir speed of 6.5. 4.36 grams of iron nitrate (FE $(NO_3)_3$*$9H_2O$) is measured out and stirred into 15 mL of DI water. This solution is added to the TEOS solution, and the combined solution is stirred for an additional 20 minutes. Finally, two drops of nitric acid are added to the solution, and allowed to stir for 15 more minutes. The solution is then allowed to sit for 24 hours.

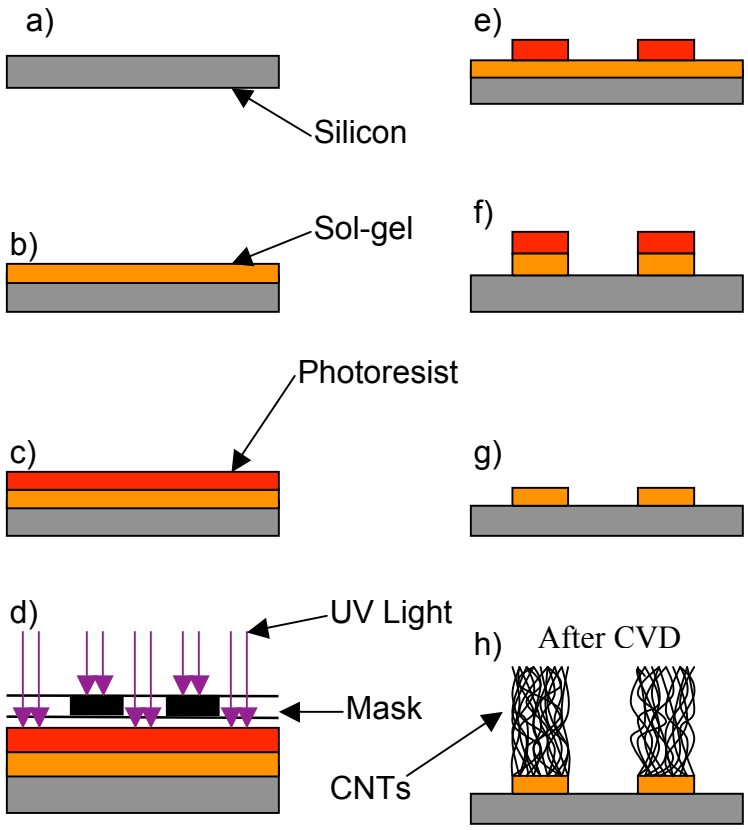

Figure 2.1 - Outline of the sol-gel deposition process.

A silicon wafer upon which the VACNT turf goes through some initial cleaning steps before sol-gel deposition begins. First, the sample is 5-step cleaned, a process where the wafer is rinsed in 5 rapid steps, with acetone, isopropyl alcohol, DI water, and then again with acetone and isopropyl alcohol, and then finally blown dry with nitrogen. This process removes organics from the surface of the wafer. Next, the silicon wafer is placed in buffered oxide etch (BOE) etching to make sure that any thermally grown oxide is removed. BOE is a buffered solution of hydrofluoric acid, which preferentially etches silicon oxide, while doing minimal etching to elemental silicon.

As outlined in Figure 2.1, the wafer is placed on a wafer spinner (a). The sol-gel is deposited on the wafer with a filtering syringe (b) that filters out any large particles that may have ended up in the sol-gel solution. The wafer is spun at 3000 rpm for 30 seconds, and then placed on a hotplate at 90 °C for a minimum of 8 hours. After the sol-gel is allowed to cure, hexamethyldisilazane (HDMS) is spun on the wafer at 3000 rpm for 30 seconds. HDMS is a binding agent that allows photoresist to adhere more effectively to the silicon wafer. This is followed by spinning AZ 5214 photoresist at 3000 rpm for 30 seconds (c). AZ 5214 is a positive photoresist, meaning that any area exposed to UV light will become soluble in developing solution.

A mask is manufactured in the desired format for the VACNT turfs, be it a series of individual arrays, single turfs, or any other desired configuration. This mask is placed over the wafer, and any exposed photoresist is exposed to UV light for 12 seconds (d). The wafer is placed in 4:1 DI water:AZ400K developer to remove any UV exposed photoresist (e). Upon placement in BOE solution, the sol-gel not covered by remaining

photoresist is removed (f). The remaining photoresist is then rinsed away with acetone, leaving patterned sol-gel (g). Carbon nanotubes grow on the patterned sol-gel through chemical vapor deposition (h).

2.3 Chemical Vapor Deposition Process

The patterned silicon wafers are placed in a CVD chamber, owned by our collaborators at Portland State University.[1] The wafers go through a series of calcination and activation steps before growth finally occurs. The calcination step occurs at 450 °C for 120 minutes at a pressure of 0.4 mBar. The activation stage occurs at 100mBar, with 385sccm of H_2 flowing through the chamber. This stage takes 90 minutes, with a ramping of temperature from 500 °C, to 600 °C, to 750 °C taking place at 30 minute intervals. Finally, the growth stage occurs, with 25 sccm of C_2H_2 flowing through the chamber along with the 385 sccm H_2. This stage lasts for 30 minutes.

The ~10nm iron nanoparticles lying on the sol-gel behave as a catalyst. The catalytic nature of the iron and the 750 °C temperature cause the C_2H_2 to dissociate upon contact with the nanoparticle. The carbon is absorbed into the nanoparticle, while the hydrogen escapes the chamber. The carbon in the nanoparticle will reach a saturation point as more carbon enters the particle. The saturated carbon will flow to the surface of the particle and form into a CNT.[2]

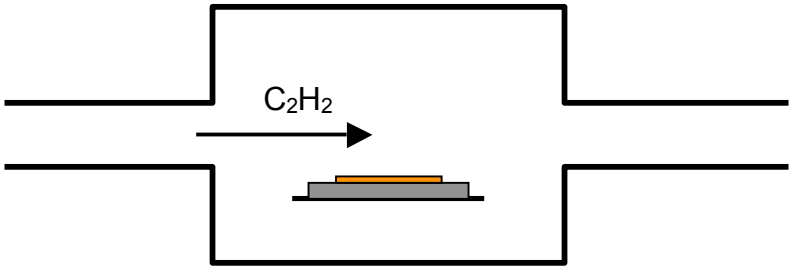

Figure 2.2 - Diagram of a CVD chamber

There are two different growth mechanisms observed during the growth of CNTs using CVD, as a result of the strength of the adhesive bond between the iron nanoparticles and the sol-gel substrate. If the iron nanoparticle is adhered strongly to the sol-gel substrate, as the carbon supersaturates and forms a CNT, the CNT will grow out of the top of the iron nanoparticle, while the particle remains adhered to the sol-gel. This is referred to as base growth.[3] When the iron nanoparticle is not well adhered to the sol-gel surface, the growth occurs at the bottom of the carbon nanotube, the nanoparticle breaks away from the sol-gel, and follows the tip of the CNT as it grows. This is referred to as tip-growth.[3] A diagram of the two different growth mechanisms is shown in Figure 2.3. An SEM image in Figure 2.4 demonstrates tip-growth. The metallic nanoparticle, due to easily released secondary electrons, will show up brighter than a CNT.

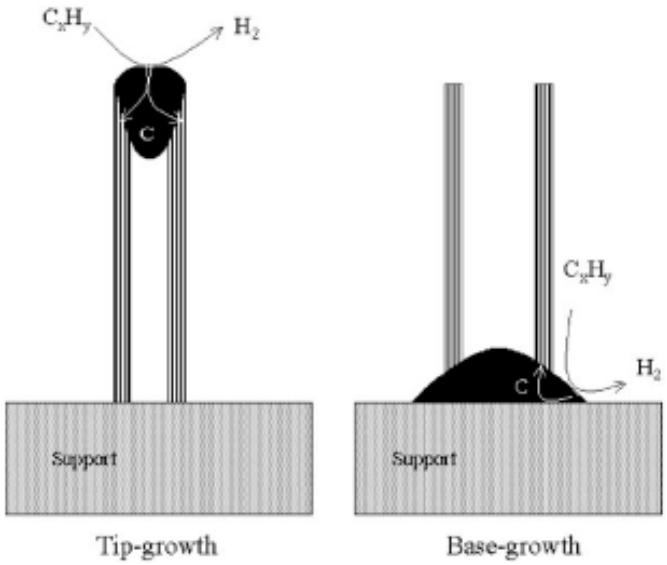

Figure 2.3 - The two growth mechanisms for CNT growth during chemical vapor deposition. From Dupuis.[3]

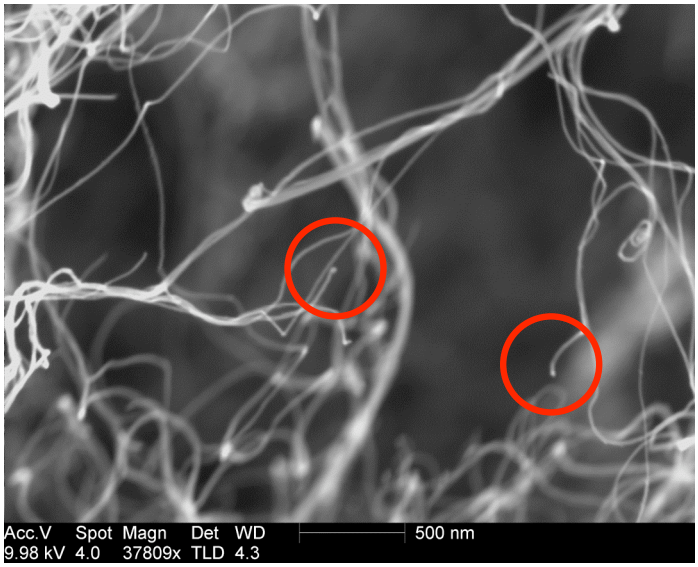

Figure 2.4 - CNTs within a VACNT turf. The red circles indicate tip growth.

2.4 Tungsten-carbide probe experiment

Initial experiments were conducted to explore the effects of the contact area on the electrical resistance of a VACNT turf using of a contacting probe. As diagrammed in figure 2.5, a tungsten carbide probe was brought above the turf (a), and then brought into contact with the top of the VACNT turf, and another tungsten carbide probe was touched on the blank wafer near the turf (b). Resistance measurements gave a value of ~130 kΩ. The tip was then brought up from contact (c) and brought into contact again (d). Resistance during the second contact has been an average of ~500 kΩ higher than the first measurements. In an attempt to discover why the resistance increased on the 2nd contact, the tungsten tip was imaged using Scanning Electron Microscopy, and are shown in Figure 2.6. This result demonstrates the adhesive properties of carbon nanotubes, due to strong local Van der Waals interactions. Unless the stickiness is suppressed by reducing local Van der Waals forces, carbon nanotubes are not useful as thermal switches.

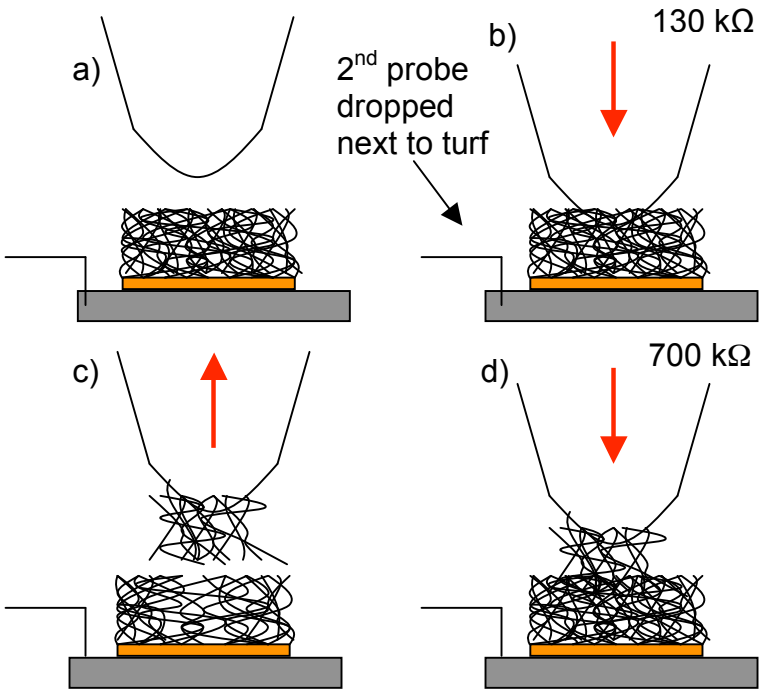

Figure 2.5 - Electrical measurement of uncoated VACNT turf using a tungsten-carbide probe

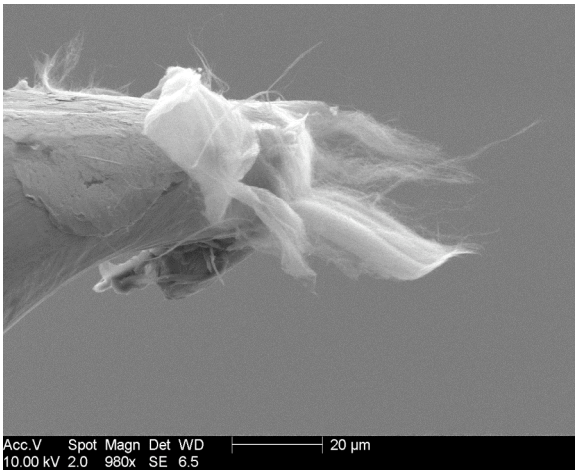

Figure 2.6 - CNTs from a VACNT turf, adhered to a tungsten-carbide probe

2.5 Mechanical transfer of VACNT turfs

A major issue in the application of VACNTs as a thermal switch in MEMS devices is the high temperature required for VACNT turf growth. VACNT turf growth using CVD requires temperatures around 750 °C. The construction of the heat transfer device is often one of the final phases in MEMS construction, and 750 °C temperatures will usually result in damage to the device. Thus, in order for VACNT turfs to be useful in MEMS and microelectronics, the VACNT turf must be grown separately and then mechanically transferred to the device at a much lower temperature, as shown in Figure 2.7.

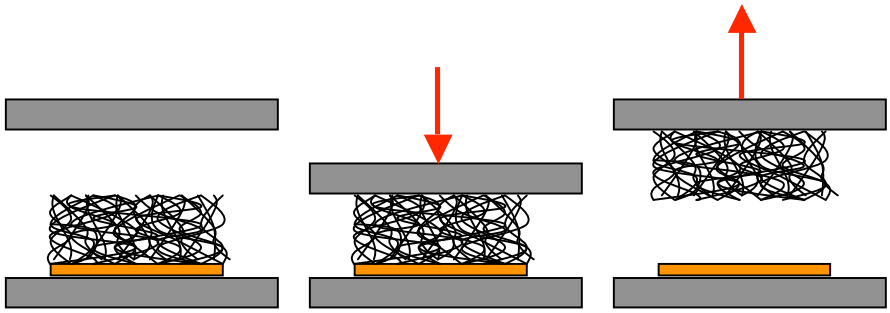

Figure 2.7 - Concept of mechanical transfer of a VACNT turf

Tests were first conducted to see if it was possible to transfer a bare VACNT turf to a bare silicon wafer at room temperature, as diagramed in Figure 2.7. The top of the VACNT turf was brought into contact with a bare silicon wafer and the structure was compressed. A major goal in the mechanical transfer of VACNT turfs is to cause as little damage as possible to the VACNT turf. As shown by Zbib in the previous chapter,

VACNT turfs buckle, and the stress required to cause buckling of the turf is dependant on the height of the turf. Thus, the maximum amount of force able to be applied to the structure is chosen based on the height, to minimize damage to the VACNT turf.

The first tests used compression that was well below the buckling stress, with the goal of trying to mechanically transfer turfs with minimal damage to the turf. For this purpose, no extra weight was placed on the structure, and only the weight already provided by the silicon wafer was used, which led to a small stress of 0.75 kPa. This structure was placed in a furnace at 350 °C for four hours. No transfer was observed in the attempts to transfer a bare VACNT turf to a bare silicon wafer. If any bonding occurred between the top of the VACNT turf and the silicon wafer, as should be expected due to the observance of Van der Waals interactions, the bonding was insufficient to overcome the strength of the bond between the VACNT turf and the sol-gel substrate.

Zbib *et al* demonstrated that a thin film of gold reduces Van der Waals interactions with CNTs and makes VACNT turfs more compliant, which are ideal properties for thermal switches. The characterization of the effects of a gold film, including the morphology of the top of the VACNT turf, has led to the idea of taking advantage of the gold film in the attempts to mechanically transfer VACNT turfs. The idea is to use heat, pressure and time to create bonding through diffusion, and make the bond strong enough that when the structure is pulled apart, the bond is stronger than the bond between the VACNT turf and the sol-gel, breaking that bond and allowing transfer to occur.

The second test brought a VACNT turf sputtered with a 5 nm TiW adhesion layer and 300nm of gold into contact with an uncoated silicon wafer and heated at 450 °C for

one hour. The TiW layer has been shown to strengthen the bond between a gold film and its substrate. For all subsequent experiments where a gold film is sputtered, a 5 nm TiW layer is first deposited. For this experiment, as previously out of concern for damage to the VACNT turf, the test was conducted without any weight being placed on the structure. The total weight on the VACNT turf was equal to the weight of the uncoated silicon wafer, which applied a stress of 0.75 kPa, well below the buckling stress of the VACNT turf. Two transfers were attempted in these conditions, and neither of them produced any transfer. Another run was attempted at a temperature of 750 °C for 3 hours, in an attempt to increase the rate of diffusion bonding. This produced no transfer, and ended up causing damage to both the turf and the gold film, due to the high temperature, as shown in figure 2.8. The gold/silicon binary phase diagram revealed that gold and silicon are eutectic at 380 °C. This produces an upper temperature limit for the use of gold films as a mechanism for thermocompression bonding to a silicon wafer.

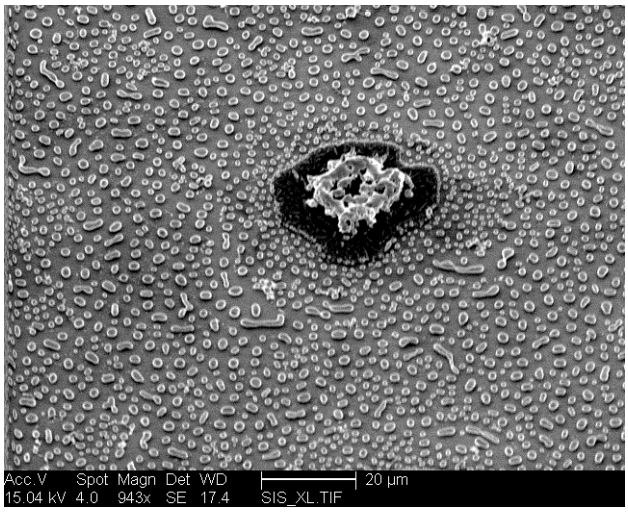

Figure 2.8 - Damage to a VACNT turf array still on its original substrate after attempted mechanical transfer at 750 °C

With the temperature restrictions put in place by the eutectic temperature of gold and silicon, and the further temperature restrictions required for mechanical transfer of VACNT turfs to be useful in MEMS applications, gold was temporarily discarded as the metal of choice. Due to low melting temperature, tin was selected as a candidate for mechanical transfer.

Tin has a melting point of 232 °C, making it a viable candidate for mechanical transfer, due to its ability to diffusively bond at lower temperatures. A VACNT turf was coated in 300 nm of tin, and then brought into contact with a silicon wafer, also coated in 300 nm of tin. The sample was left in a furnace at 210 °C overnight, totaling 18 hours. The process resulted in no transfer. An odd occurrence during the transfer attempt was a discoloration of the film. It was realized that, since the heating occurred in ambient air, the tin was oxidizing.

The oxidizing of the tin film proved to be detrimental for mechanical transfer. In order to use tin, oxidization has to be prevented, by doing mechanical transfer either in an inert environment or a vacuum. Even if oxidation is controlled during processing, it also leads to an issue with usage of the device as a thermal switch. Any oxidation of the film during usage of the device will lead to the device becoming ineffective, and shorten the potential lifetime of the device. This led to gold being reconsidered, due to its inertness at even very high temperatures.

Mechanical transfer tests conducted with gold films, to this point, had been attempted with very little weight on the sandwich structure, usually little more than the weight of the turf. The buckling model provided by Zbib showed that in the case of short VACNT turfs, a considerable amount of weight could be placed on the turf before buckling occurred. Therefore, the next step in trying to transfer VACNT turfs using gold films was to vastly increase the amount of weight placed on the sandwich structure. Furthermore, it has been demonstrated that transfer does not work when trying to transfer to an uncoated silicon wafer. By also coating the silicon wafer with a 5 nm TiW adhesion layer and 300 nm of gold, and placing the top of the similarly gold-coated VACNT turf against the gold film under pressure at an elevated temperature, the gold films should adhere to each other through diffusion bonding.

A 5 nm TiW adhesion layer, along with a 300 nm gold film was sputtered on a short ~20 um tall, 4x4 mm^2 turf, and brought into contact with a silicon wafer, similarly coated with 5 nm TiW and 300 nm of gold. A 450g weight was placed on the structure, much higher than the fraction of a gram of weight provided by the silicon wafer alone. The 450 g produces a stress of 1.1 MPa, which is sufficient enough to cause a lot of

buckling and damage to a tall turf, but will not damage a short turf, as shown by Zbib's buckling model in the previous chapter. With the gold/silicon eutectic temperature being 380 °C and a maximum temperature being set as a result, a new transfer temperature of 350 °C was attempted. The structure was left overnight at 350 °C, which totaled approximately 12 hours. Upon separation, the turf had transferred, as shown in Figure 2.9.

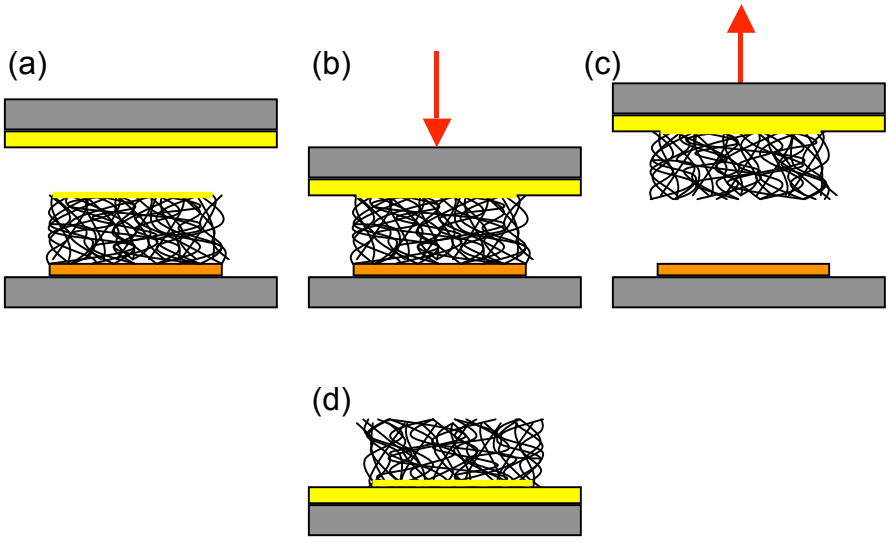

Figure 2.9 - Diagram of successful mechanical transfer using dual gold films. The sol-gel does not transfer with the turf.

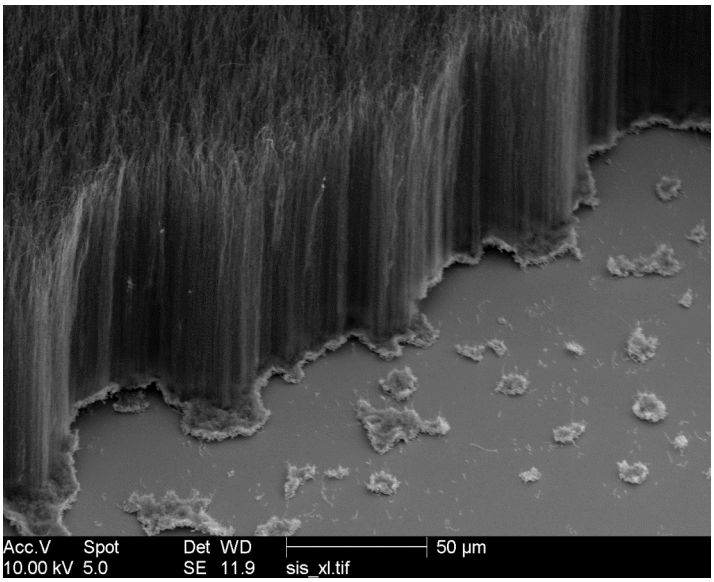

Figure 2.10 - SEM image of the side of a mechanically transferred VACNT turf

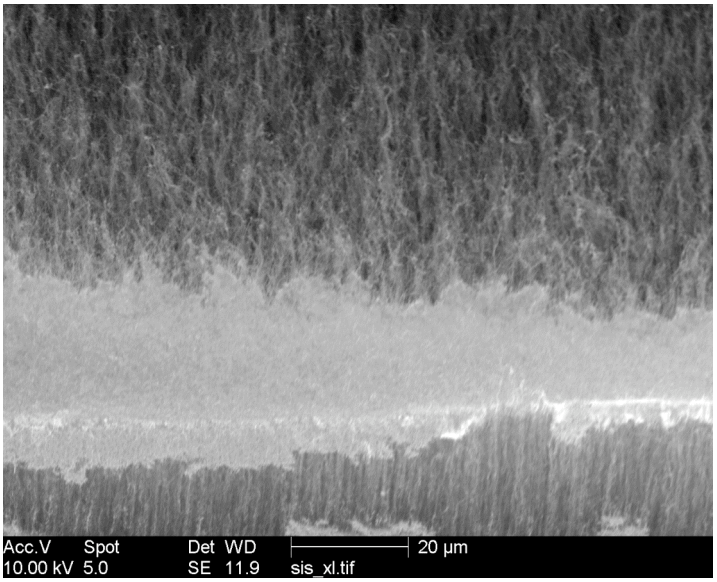

Figure 2.11 - SEM image of the top of a mechanically transferred VACNT turf where some of the sol-gel interface transferred with the turf.

The turf is now in an inverted configuration on the gold-coated wafer. The combination of heat, pressure and time causes the gold film on the silicon wafer and the

gold-coated CNTs on top of the VACNT turf to adhere to each other with a strength sufficient enough to break the bond between the bottom of the VACNT turf and the sol-gel that it grew on. The sol-gel remained on its original substrate, which is a very ideal condition for using the VACNT turf as a thermal switch, or even as an electrical switch, because the ceramic sol-gel film would no long be an impedance to conduction. There have been cases of sol-gel transferring with the turf, due to excessive stress, as shown in Fig 2.11. As long as the stress is controlled according to Zbib's buckling model, sol-gel transfer does not occur.

2.6 Optimization of mechanical transfer process

350 °C is still an excessively high temperature for MEMS devices, so it is ideal to find out how low the temperature can be taken and still allow mechanical transfer of VACNT turfs to occur. A temperature that is acceptable to MEMS devices without any damage occurring is 150 °C. A similar test to the first successful transfer was conducted, with a short VACNT turf, coated in 300 nm of gold, being brought into contact with a silicon wafer coated in 300 nm of gold. This sample was left overnight at 150 °C, totaling 12 hours. Upon separation, transfer was successful, showing that transfer could occur at temperatures as low as 150 °C.

A second issue in the mechanical transfer process that needs to be minimized is the time that the sample is compressed at an elevated temperature. Samples up to this point had been left overnight, or at least 12 hours, making the process not ideal if it is ever to reach any kind of production scale.

Samples were tested under the same circumstances as previously, with VACNT turfs coated in 300 nm of gold and then brought into contact with another silicon wafer coated in 300 nm of gold. All samples were heated to 150 °C, but instead each sample was exposed to that temperature for a varying amount of time, starting from eight hours and going down to around thirty minutes. Results of these tests showed transfer occurring with all samples greater than two hours, with minimal transfer occurring at less than two hours. Figure 2.12 shows SEM images of minimal transfer due to inadequate bonding time, showing small tufts and small spots of gold that transferred, leaving the bulk of the VACNT turf un-transferred.

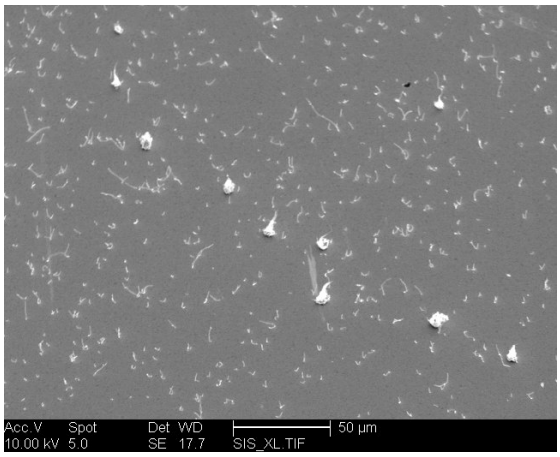

Figure 2.12 - Failed attempt at mechanical transfer of a VACNT turf due to inadequate bonding time.

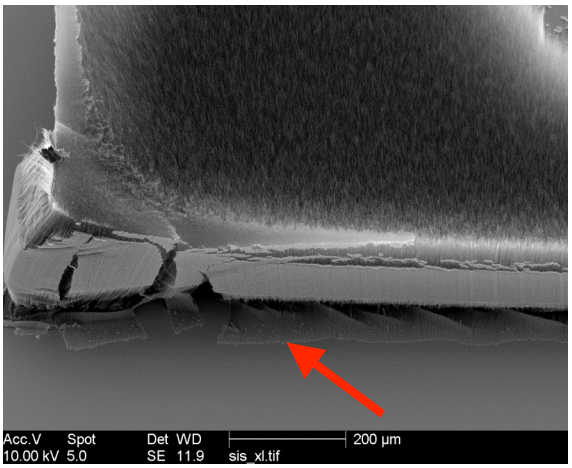

Fig 2.13 - Damage to a transferred VACNT turf due to excessive stress and buckling. The gold coated side of the turf reaches the contact surface and bonds as a result, as shown by the red arrow. Sol-gel is present along the sides of the VACNT turf.

Finally, as discussed earlier, this process should produce mechanical transfer of VACNT turfs while causing minimal damage to the turf itself. Initial tests were done with minimal weight and produced no transfer, while tests done at a weight higher than the turf's buckling stress will produce transfer, but cause damage and deformation to the turf as a result, as shown in Fig 2.13. The buckling stress for short turfs has been shown to be considerable, allowing a 0.5 kg weight, or 1.22 MPa of stress on a 4x4 mm^2 VACNT turf, to be placed on the small sandwich structure without damage to the turf. Even taller turfs on the order of ~100 um, while not able to handle the weight that shorter VACNT turfs can accept, are still able to accept weight from 50 to 100 grams, which is a weight that has been shown to be adequate enough for mechanical transfer to be successful.

Time, temperature and stress have all been taken into consideration in the attempts to optimize the mechanical transfer process. The process that has been shown to

produce consistent results is at least two hours of compression at 150 °C, using a stress just below the buckling stress of the VACNT turf.

2.7 Height variation of large VACNT turfs

A major issue in the mechanical transfer of VACNT turfs is the variation of the height across a VACNT turf, which typically occurs with large turfs. Uniform growth during the CVD process is dependant on the ability for the carbon containing gas to be able to successfully reach the sol-gel substrate as it flows over the top of the substrate. With very large VACNT turfs, the CNTs that grow near the perimeter of the turf grow as normal, but CNTs near the center of the turf do not grow as well. Figure 2.14 shows SEM images of a non-uniform VACNT turf and a diagram of what a profile of an uneven turf typically looks like.

(a) (b)

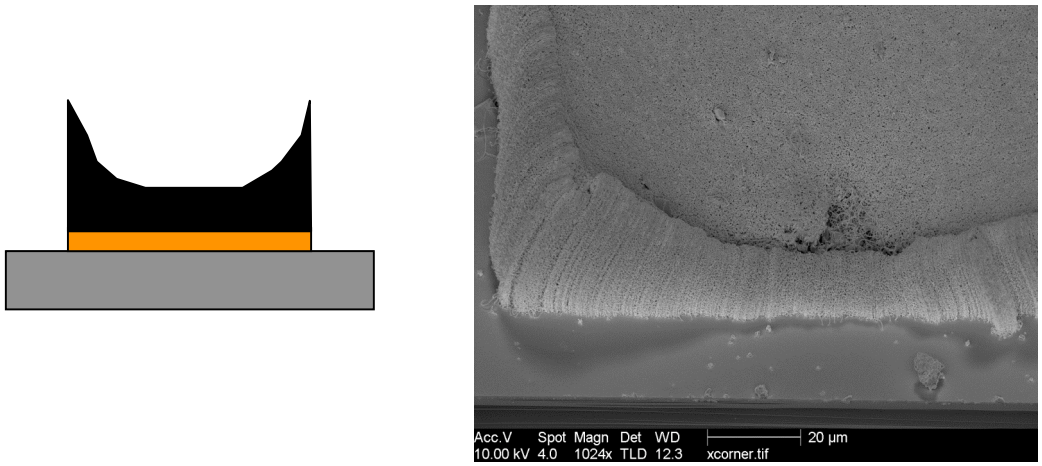

Figure 2.14 - (a) A typical profile of a large, uneven VACNT turf, where the exterior of the turf tends to grow taller than the interior. (b) An SEM image of a gold coated uneven VACNT turf

The uneven height of a large VACNT turf results in multiple issues when trying to mechanically transfer the turf. In order for the gold coated silicon wafer to make contact with the center of the turf, the exterior of the turf must be buckled down to reach the interior's height. This requires placing extra weight on the structure, damaging the exterior of the turf in the process. If, as done in prior tests, the amount of weight applied is chosen to avoid buckling of the turf, the interior of the turf will never contact the silicon wafer, and will never have an opportunity to bond. Figure 2.15 demonstrates what happens in this case.

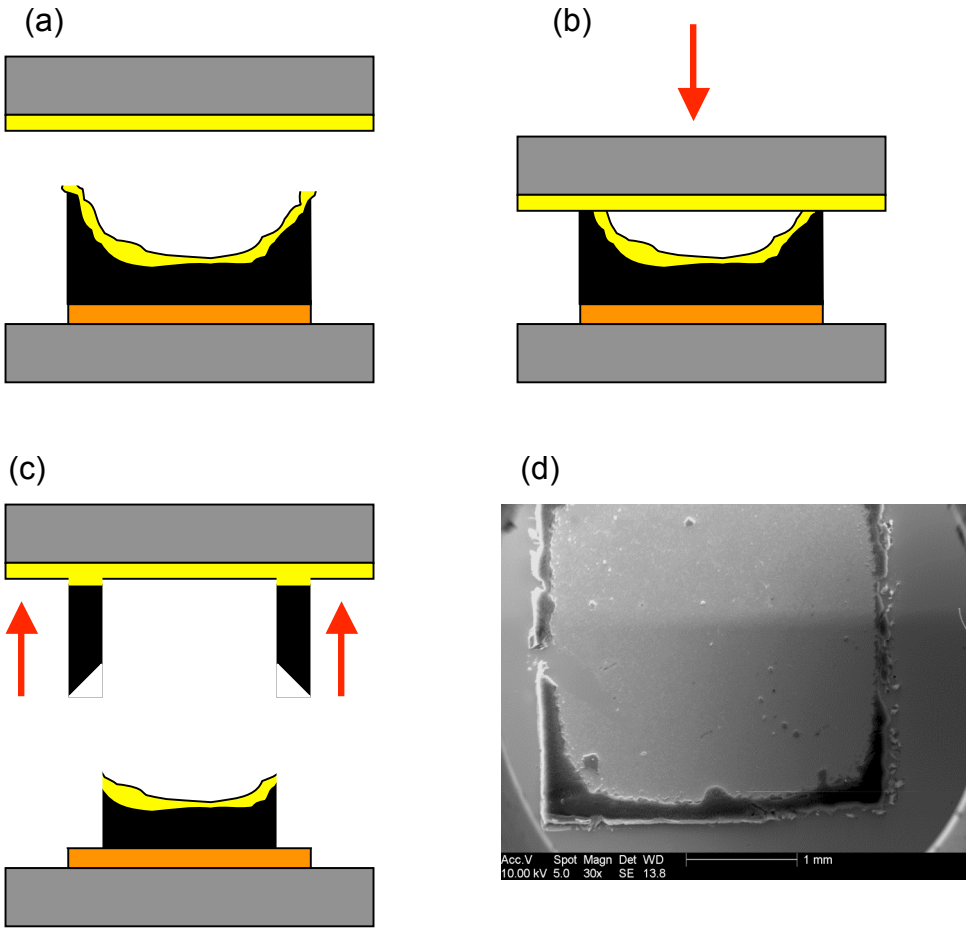

Figure 2.15 - (a) - (c) The mechanical transfer of a large non-uniform VACNT turf (d) an SEM image of the resulting transfer

A solution must be found to address the uneven turf height. A potential solution is to pattern channels in the sol-gel prior to growth, turning the large VACNT turf into an array of closely packed square arrays. This would allow the carbon containing gas during the CVD growth process to diffuse better to the center of each turf, since smaller VACNT turfs tend to not have uneven height issues, as displayed in figure 2.16, shown by Terrones. This brings in new issues with mechanical transfer of arrays, which will be

discussed in chapter four. Arrays have less lateral strength than one single turf, and are likely to "fall over" during compression, as will be shown.

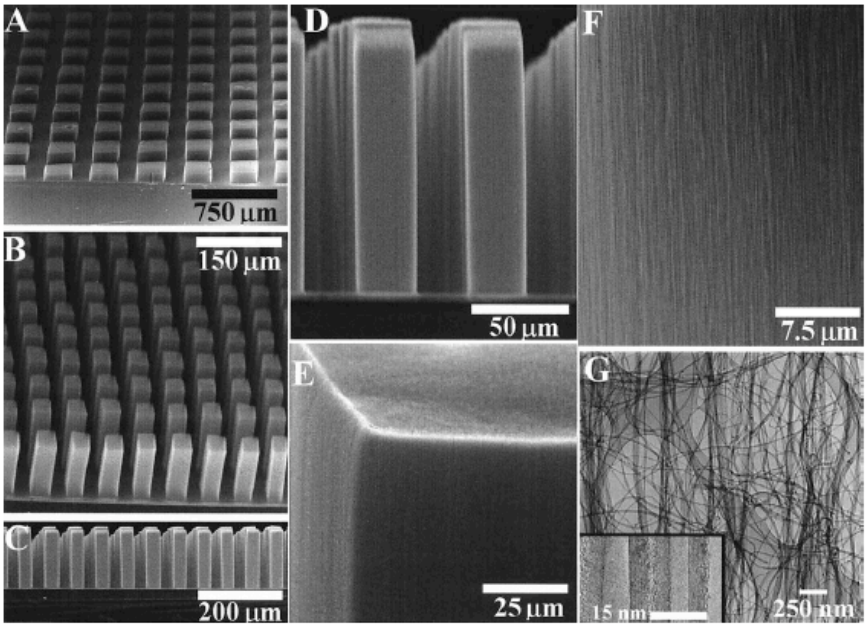

Figure 2.16 - closely packed square arrays of VACNT turfs, which can potentially overcome the non-uniformity issue demonstrated during the growth of large VACNT turfs. From Terrones.[4]

2.8 Conclusion

This chapter outlined the steps in growing VACNT turfs, including the development of the sol-gel, the sol-gel deposition process on the silicon wafers, and the growth mechanisms of CNTs in chemical vapor deposition. Initial experiments exploring the electrical properties of uncoated VACNT turfs were discussed, followed by the development of the mechanical transfer process and the parameters adjusted for successful mechanical transfer to occur. An optimization of the mechanical transfer

process was outlined, followed by a discussion of the height difference of very large VACNT turfs, and the issues in their mechanical transfer due to the non-uniform height.

The following chapter will discuss the characterization of the mechanical transfer process, including mechanical and electrical effects during separation, and will present a model for separation.

References

[1] Dong L, Jiao J, Pan C, Tuggle D W, "Effects of catalysts on the internal structures of carbon nanotubes and corresponding electron field-emission properties," Appl Phys A 78, 9-14 (2004)

[2] Seidel R, Duesberg G, Unger E, Graham A, Liebau M, Kreupl F, "Chemical Vapor Deposition Growth of Single-Walled Carbon Nanotubes at 600 °C and a Simple Growth Model," J Phys Chem B 108, 1888-1893 (2004)

[3] Dupuis A, "The catalyst in the CCVD of carbon nanotubes - a review," Prog Mater Sci 50, 929-961 (2005)

[4] Terrones M, "Science and Technology of the Twenty-First Century: Synthesis, Properties and Applications of Carbon Nanotubes," Annu Rev Mater Res 33, 419-501 (2003)

Chapter Three

3. Characterization of the thermocompression bonding of vertically aligned carbon nanotube turfs to metallized substrates

3.1 Introduction

Carbon nanotubes are a novel material with properties that make them attractive for use in thermal applications, such as thermal switches[1,2,3] and thermal interface materials[4], due to exceptional mechanical properties[5] (as they should show little mechanical wear during contact), and a very high thermal conductivity of up to 3000 W/m*K[6]. They also have possible applications in use as electrically conducting mediums, such as the MEMS micro-engine, or as a replacement materials as interconnects in microelectronics[7]. For applications that require transport over distances of μm's, it is likely that arrays or assemblages, rather than individual, nanotubes will be a useful structure. Vertically aligned carbon nanotube turfs[8] (VACNTs), also sometimes referred to as forests, are entangled, nominally vertical arrays of nanotubes, which can be either single-walled or multi-walled; one common technique for fabricating these structures is chemical vapor deposition (CVD)[9]. The temperature required for growth of VACNTs using CVD is often approximately 700 ºC[10,11]. The high temperatures required for growth may limit the ability to grow VACNTs directly onto a microelectronic device or microelectromechanical system (MEMS). To separate the thermal budget for the growth conditions from the possible limits in processing temperatures in electronic and MEMS applications, it would be beneficial to be able to transfer a patterned array of VACNTs to a different substrate for use in a complete system.

Several different methods of VACNT transfer between the growth substrate and another substrate have been demonstrated by a range of research groups. In general these have focused on the ability to transfer a VACNT array from a broad turf to a patterned media. These include transfer using a low temperature solder[12], transfer onto polymer films[13], "dry contact transfer" onto polymeric adhesive tape[14], and a wet transfer method[15]. In all these cases, the VACNT is grown, and then transferred to a different substrate. The substrate it is transferred to is most likely stiffer elastically than the VACNT array, as similar VACNT structures have been shown to have a tangent elastic modulus of 10-20 MPa[16].

This paper outlines a solid-state transfer process of thermocompression bonding VACNTs to metallized semiconductor surfaces, such as those that might be found in either thermal or electrical contact applications. As optimized in the previous chapter, this process allows for the direct transfer at 150 ºC of separately grown VACNTs to other silicon based metallized substrates, a temperature within the acceptable thermal budget of MEMS or semiconductor processing[17]. Separation stresses of interfaces are characterized, along with the electrical resistance of the bonded VACNTs. Finally, a model of separation during mechanical transfer is presented.

3.2 Fabrication and Experimental Procedures

VACNTs were grown using a sol-gel catalyst suitable for photolithographic patterning and subsequent CVD[11]. The CVD process in this study produces multi-walled carbon nanotubes (MWCNTs). To briefly summarize the growth conditions, detailed in the previous chapter, a TEOS based sol-gel containing iron nitrate was spun onto boron

doped silicon wafers, and then patterned using photolithography. The pattered samples are heated to 750 °C, whereupon Fe precipitates in the glass phase, leading to 10-20 nm particles which act as catalysts for CNT growth[16]. The CNTs grow in a nominally vertical direction. The pattern used for these experiments was a square, 4 mm on a side; this method has previously been used to pattern VACNTs to dimensions of less than 5 μm on a side[18].

For each sample, an FEI Sirion SEM was used to measure the height of the CNT turf. The thickness of the VACNT varied from sample, and ranged between 20 and 100 μm. The nominal volume was simply calculated from the area and thickness measurements. To quantify the nominal density of the VACNT, the nominal volume of the turfs was measured, and then the turf was removed from its substrate, and the weight difference was measured using the scale of a Perkin-Elmer TGA, which has a sensitivity of 0.1 μg. These measurements are used to calculate the density of the CNT turf.

The top of the CNT turf was sputter coated with a 5 nm TiW adhesion layer and then a nominally thick 300 nm Au film. This sputtering does not form a uniform gold film on top of the turf. Rather, the gold encapsulates the individual nanotubes or small clusters of tubes. Micrographs of the top surface of the patterned and gold-coated structures are shown in Figure 3.1.

The gold encapsulated top of the turf was then brought into contact with an oxidized silicon wafer, similarly coated with a 5nm TiW adhesion film and a 300 nm Au film, forming a sandwich structure. Thermocompression bonding was used to bond the gold layers together. The structure was compressed with a load appropriate to generate a nominal stress in the turf sufficient to cause, but not exceed, the buckling stress, which is

dependant only on the height and effective elastic modulus of the turf[19]. In most cases in this paper the applied load was between 0.5 and 5 N. The sample was then heated to 150 ºC in ambient laboratory air. A minimum of two hours was required to make the Au/Au interface sufficiently strong to allow mechanical transfer, meaning that the Au/Au interface was stronger than the interface between the sol-gel and the base of the VACNTs, referred to as the sol-gel interface. These steps are shown schematically in Figure 2**,** along with an optical photograph of the bonded structure.

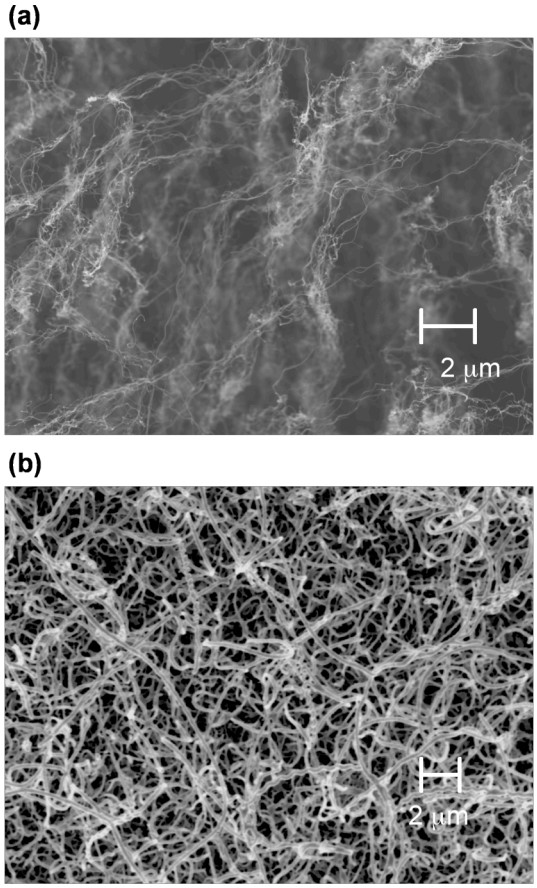

Figure 3.1 - Top view of as grown (a) and gold-coated (b) VACNTs showing general morphology of the structure.

An electrical connection using conductive epoxy was formed on the gold film on both silicon wafers, establishing an electrical circuit through the VACNTs that bypass the silicon wafers. The bonded sandwich structure was placed into an electromechanical test stand in which one silicon die (the "top") was fixed to a rigid aluminum frame, and a tensile load was applied to the structure by moving a two-prong fixture with a Parker stepper motor, and hence imposing a fixed displacement rate of 4 μm/s, to the "bottom" die, effectively pushing the bottom die away from the fixed "top" die. This is shown schematically in Figure 3.2c. The applied load was monitored using a Honeywell miniature load cell. The nominal stress (the applied load divided by the original nominal area defined by the pattern), as well as the electrical resistance of the turf, was monitored as a function of displacement as the turf was separated. The voltage across the turf is measured during separation. A 24.3 Ω resistor was placed in series with the sandwich structure, and a 1 V potential is placed across the circuit using a Hewlett Packard DC power supply. Current through the turf can be calculated by measuring the voltage across the resistor. The resistance of the turf can then be directly determined from the current-voltage measurements.

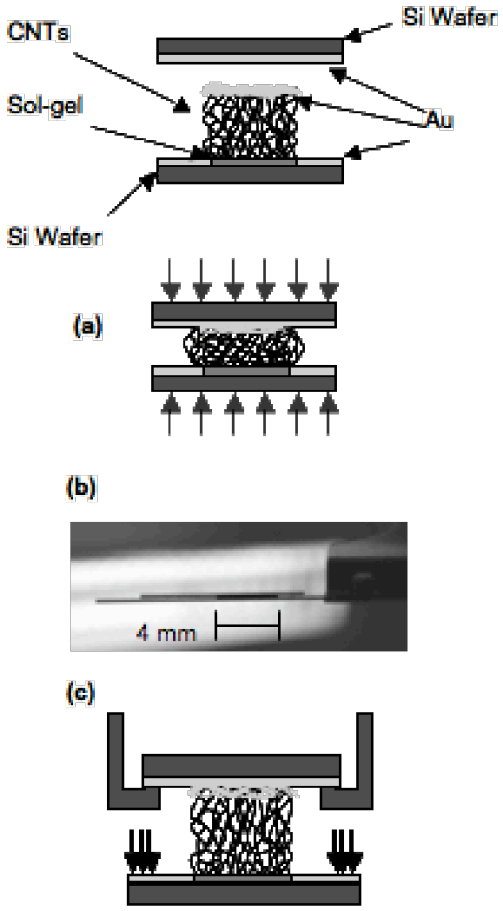

Figure 3.2 - (a) Thermocompression bonding of a CNT turf at 150C for >2 hrs. (b) An optical image of the sandwich structure profile. (c) Schematic of separation process, with the top wafer fixed and a normal force applied to the bottom wafer.

After the silicon die sandwich structure has been separated, inspection of the interface showed that the sol-gel interface fails, and the turf has transferred to the Au-coated wafer. The sol-gel is left on the original substrate, and VACNTs are inverted from their original position on the Au-coated wafer. Using this structure, where the gold coated top of the VACNTs are now the base for the next bonding step, the VACNT is again coated with nominally 5nm TiW and 300 nm Au, and then thermocompression bonded with another gold coated silicon wafer with the same thickness layers. Upon

completion of this step a complete double Au/Au interface sandwich structure (SiO_2–TiW-Au-Au-TiW-VACNT-TiW-Au-Au-TiW-SiO_2) has been formed.

The separation from the solgel characterizes the strength of the solgel interface, but does not indicate the strength of the Au-VACNT bond, except that it is stronger than the solgel interface. To characterize the strength of the gold interface, the complete sandwich structure was tested in tension while monitoring the electrical resistance of the structure.

3.3 Results and Discussion

The CNT array is shown before and after the transferring process in figure 3.3, where position (A) in figure 3(a) is the same location as position (A) in figure 3.3b. To verify electrical conductivity, an *I-V* curve was performed on the bonded structures. Two typical curves from two separate samples are shown in figure 3.4; the linearity of the curves suggest metallic behavior in the VACNTs used in this study. Both turfs were 50 μm thick and had nominal areas of 8.7 and 16 mm^2 projected area; therefore the conductivity of the turfs are 2.1 and 1.2 S/m, respectively. The conductivity varied significantly between samples; values between 1 to 50 S/m were measured on samples in this study, though the conductivity of a given sample was reproducible. Work reported by Kang[20] on MWCNT turfs shows conductivity on the order of 10 S/m, similar to this current study. The nominal density of our VACNT turfs is ~0.13 g/cm^3, with density values ranging from 0.016 to 0.232 g/cm^3. This is consistent with density measurements conducted by Wang *et. al*[21], who reported a density of 0.032 g/cm^3. SEM images of the rough morphology of the CNT turfs and this low density suggest that the actual contact

area is much lower than the nominal area, and therefore it is to be expected that the actual electrical conductivity of the individual tubes are substantially higher than calculated using the nominal areas. The *I-V* curves both show an electrical resistance of 2.7 Ω; the typical electrical resistance of the sandwich structures is ~2 Ω.

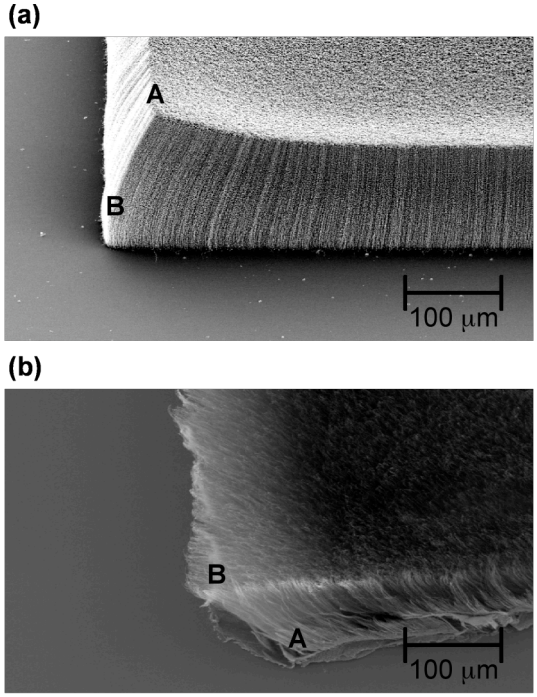

Figure 3.3 - A corner of an Au coated CNT turf prior to transfer (a), and the same corner after mechanical transfer on a different substrate (b). The letters correspond to equivalent points.

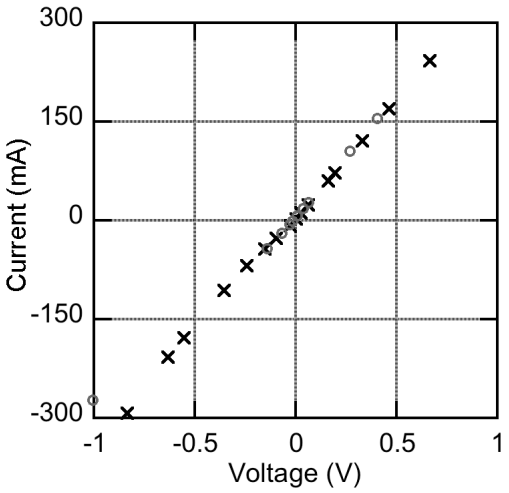

Figure 3.4 - I-V curves for two different sandwich structures (open circles and x's) with Au/Au interfaces on both sides of the CNT turf.

The nominal tensile stress and resistance was measured as a function of displacement during separation from the underlying catalyst layer, as shown in figure 3.5 for a typical sample**.** The behavior is non-linear, and can be separated into four different regions of behavior, shown schematically in figure 3.6. First, previous research has shown that during compression the VACNT buckles[19]; therefore we suggest that the initial tensile load results in a reversal of the barreling or buckling that took place during thermocompression bonding. With continued tensile loading, it is reasonable to expect a straightening of the relatively tortuous topology of the nanotubes will occur, corresponding with a change in the slope of the stress – displacement curve. The stress reaches a peak, referred to as the separation stress, noted as position (3) in figure 3.5, and it can be assumed that at this point nanotubes start detaching from the sol-gel surface (as the strength of individual CNTs has been demonstrated to be orders of magnitude greater

than this nominal stress, and even higher than that if the stress was calculated using an area that was scaled to the density of the VACNT compared to a single CNT). In region four, with decreasing loads and nominal stresses with increasing displacement, the nanotubes continue to separate from the sol-gel and the turf is fully transferred.

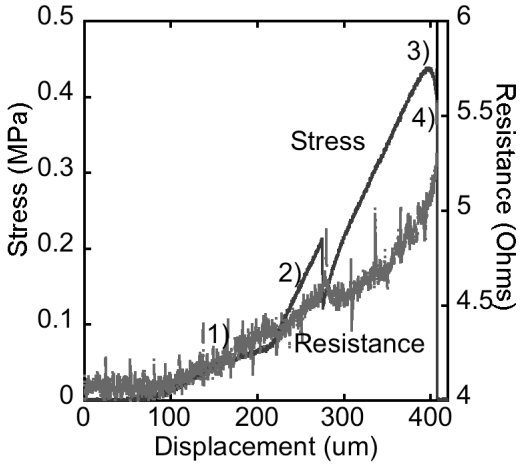

Figure 3.5 - Stress and electrical resistance vs displacement during mechanical transfer of a CNT turf off of its original sol-gel substrate. Labels correspond to different regions of behavior by the CNT turf during separation. Electrical resistance goes to infinity upon separation.

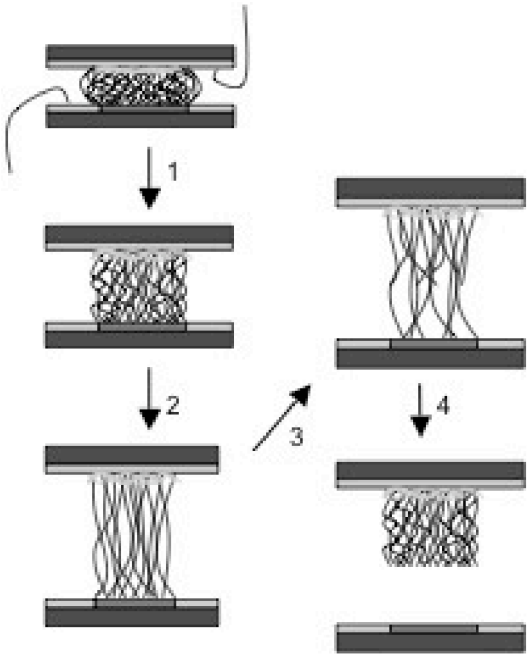

Figure 3.6 - Mechanical transfer of a VACNT turf from its sol-gel substrate, also showing where electrical leads are connected. Four proposed mechanisms of behavior are noted, which correspond to the labels on Fig 3.5.

The increase in electrical resistance during the buckling reversal and straightening phases of separation can be attributed to detangling of the CNTs. We believe that many CNTs terminate within the turf without ever reaching the contact surface. This would lead to those CNTs being unable to contribute to the resistance of the turf unless they are interacting with nearby nanotubes that reach the surface. There is a further increase in resistance when the separation stress is reached, as CNTs begin to detach themselves from the solgel, decreasing the actual contact area and the number of CNTs available to conduct electrons. The increase in the electrical resistance during the entire pull-off process from the sol-gel is ~1 Ω, which is a 20% increase.

Similar measurements were conducted with the complete sandwich structure where each side of the turf has an Au/Au interface. Figure 3.7 shows the stress and electrical resistance as a function of displacement for the separation of a sandwich structure consisting of a 20 μm tall CNT turf with Au/Au interfaces on both side of the turf. First, note that the nominal strain in the structure is between 200 and 300%; even if the weight of the sample and thermocompression bonding had shortened the VACNT to an infinitesimal thickness the sample has extended at least twice it's original height.

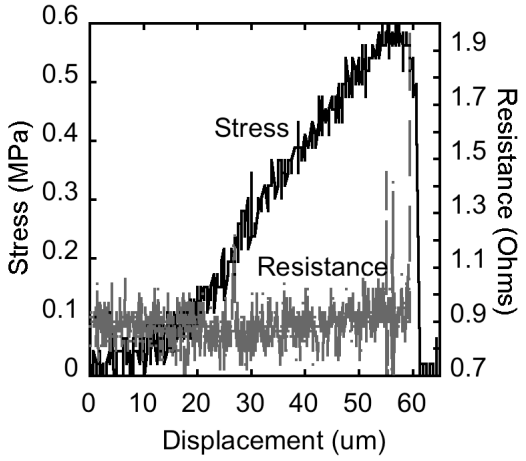

Figure 3.7 - Stress and electrical resistance vs displacement during separation of a sandwich structure with Au/Au interfaces on both sides of the CNT turf.

While Figure 3.7 demonstrates a similar mechanical response for the separation of a turf being pulled off of the sol-gel layer, the electrical response is very different. The electrical resistance is a factor of four lower than the initial separation from the sol-gel. This should be expected, since there is no insulating sol-gel layer. In this structure, however, the change in resistance during separation is an order of magnitude less than the resistance change when the turf is being pulled off of the growth substrate. The Au

coating electrically links all of the tubes with each other, while in the case of the solgel structure the nanotubes on the solgel side of the sandwich structure are electrically isolated from each other by the oxide. This places more importance on the entangled linking between the nanotubes within the turf. With the Au/Au structure, the detangling of the nanotubes during separation has less of an effect on the conductivity than the original transfer, since the gold film already links them to each other. There is still a slight increase in resistance after the separation stress is reached, due to a decrease in contact area.

Twelve samples were transferred from the sol-gel layers to an Au coated wafer, and six of those were then successfully bonded to another wafer. It is to be expected that the average separation stress for an Au/Au interface is higher than the separation stress off of the sol-gel. Transfer from the sol-gel results in an average nominal separation stress of 0.42 MPa, where the total range of measured stresses was from 0.08 to 0.58 MPa, while the average separation stress for an Au/Au interface is 0.553 MPa with a range spanning 0.26 to 0.88 MPa.

The final separation in the complete Au/Au sandwich structure can be complex. One Au/Au interface may be stronger than the other, or both may have similar strengths. This results in cases where the turf may transfer to either one or the other substrate, or parts of the turf stay on both substrates. In some cases, tufts of a turf may transfer, while the bulk of the turf does not transfer. The tensile strengths of this interface do not show a Gaussian distribution, and hence the difference between the two lots of samples (stress required to remove the sample from the growth substrate, and the stress required to separate the sandwich structure) was analyzed using a Wilcoxon statistical analysis[22], the

result of which gives a p-value of 0.07. Statistical significance is generally assumed when p is less than 0.05, so we cannot conclusively state that the connection is statistically significant, though the higher mean value for separating the bonded structures in the complete sandwich structure are what would be expected for this transfer technique.

The sandwich structures were prepared and separated in batches, with the initial bonding and sol-gel pull-off occurring in a batch along with other samples. The batch of transferred turfs was then sputtered with gold, bonded with a gold-coated wafer, and then separated to get measurements of the Au/Au interface failure. Because of the batch process, the individual turfs were not tracked between their sol-gel pulloff and their Au/Au interface test, although it was possible to track the samples. One sample was tracked through both its sol-gel pulloff and the Au/Au interface pulloff. The separation stresses were 0.58 MPa and 0.62 MPa, respectively, lending further credence to the assumption that the Au/Au interface is stronger than the sol-gel interface.

The bonded structure can potentially fail in four different places. The likely failure locations, shown schematically in Figure 3.8, include (1) failure of the nanotube itself; (2) an "unsheathing" of the nanotube from its gold encapsulation; (3) a failure of the thermocompression bond between the Au/Au interface; and (4) a delamination of the Au film from the Si wafer. Electron microscopy observations of the failed interfaces showed that the bond typically failed at (3), the Au/Au interface, also shown in Figure 8. There should rarely be a failure under conditions (1) or (4) noted above, as the level of applied nominal stress is extremely unlikely to cause failure of the nanotube or

delaminate the Au film from the Si substrate, and indeed we did not observe any evidence of failure modes (1) and (4), and only rarely observed (2).

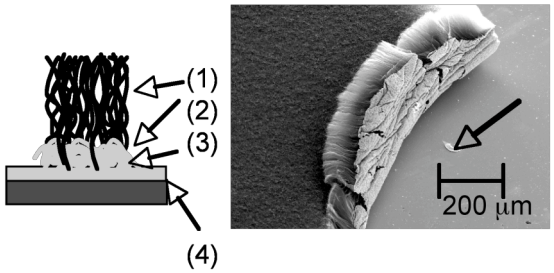

Figure 3.8. Potential failure points of the Au/Au interface: Failure of the nanotube (1). "Unsheathing" of the nanotube from its Au encapsulation (2). Failure of the thermocompression bond (3). Delamination of the Au Film (4). Arrow on SEM image indicates (2) type failure, while the majority of failure falls under the type (3) behavior.

Several unique features of using VACNTs as conductive interface materials can be noted from this study. First, the electrical resistance of the structures was not significantly dependent on the nominal density of the turf. When compressed on the order of 50%, based on the applied stresses noted from previous work[19], and when extended by up to 200%, the conductivity was effectively constant to within the range of our measurements. This is similar to the results of work by Yaglioglu[23], who monitored the conduction during contact of gold sphere into a VACNT. Changes in their contact resistance could be interpreted as solely linked to changes in contact area of the sphere. Therefore, improvements in conductivity must focus either on increasing the actual growth density (more CNTs per square mm of growth surface) or in reducing the contact resistance of the structures. Secondly, the VACNT structure is robust even when buckled

and deformed, and with moderate applied loads the device can be "straightened". This also suggests that changes in dimension due to thermal expansion mismatches will be low, as the modulus of the VACNT is much lower than most semiconductor packaging materials and will be elastically deformed to accommodate their dimensional changes during loading, as well as providing some latitude in the process of thermocompression bonding. Finally, the compliance of the coated structure was tied closely to the ability to thermocompression bond the device. Only nominal stresses near the buckling stress were able to successfully bond the device as constructed. Longer times at lower stresses using the same bonding temperature were unable to successfully transfer the VACNT from the growth substrate to the metallized wafer; suggesting the interplay between mechanical and thermal diffusion processes will need to be examined in more detail.

3.4 Conclusions

This paper introduces a new technique that allows dry mechanical transfer of VACNTs at 150 °C to metallized substrates using thermocompression bonding. This process allows for VACNTs to be grown separately and then be mechanically transferred to a device within an acceptable thermal budget for most microelectronics and MEMS devices. The process can form either a contact switch for electrical or thermal switching (i.e. after the first transfer step), or, once a complete sandwich is formed, a permanent conductive interface (such as an electrical or thermal interface material). The nominal strength of the VACNT to the sol-gel growth layer was 0.42 MPa, whereas the nominal strength of the Au coated VACNT to an Au coated substrate was 0.53 MPa. The compressed interface was shown to have non-linear mechanical behavior, likely linked to

un-buckling of the initial buckled turf, the straightening of the individual tubes, and the subsequent separation from the substrate by individual tubes. The change in electrical resistance during separation was minimal; in the case of the Au-CNT-Au couple less than a 10% increase in electrical resistance was observed even with a greater than 200% elongation of the turf's nominal height. This suggests significant flexibility in the assembly and use of these conductive layers.

References

1. Weiss L W, Cho J H, McNeil K E, Richards C D, Bahr D F, Richards R F, "Characterization of a dynamic micro heat engine with integrated thermal switch," J Micromech Microeng 16, S262-S269 (2006)
2. Christensen A O, Jacob J P, Richards C D, Bahr D F, Richards R F, "Fabrication and characterization of a liquid-metal micro-droplet thermal switch," Transducers, Solid-State Sensors, Actuators and Microsystems, 12th International Conference 2, 1427-1430 (2003)
3. Cho J, Richards C, Bahr D, Jiao J, and Richards R, "Evaluation of contacts for a MEMS thermal switch," J Micromech Microeng 18, 105012 (2008)
4. Xu J and Fisher T S, "Enhancement of thermal interface materials with carbon nanotube arrays," Int J Heat Mass Tran 49, 1658-1666 (2006)
5. Treacy M M J, Ebbesen T W, Gibson J M, "Exceptionally high Young's modulus observed for individual carbon nanotubes," Nature 381, 678-680 (1996)

References

6. Kim P, Shi L, Majumdar A, McEuen P L, "Thermal Transport Measurements of Individual Multiwalled Nanotubes," Phys Rev Lett 87, No 21 215502 (2001)

7. Kreupl F, Graham A P, Duesberg G S, Steinhögl W, Liebau M, Unger E, Hönlein W, "Carbon nanotubes in interconnect applications," Microelectron Eng 64, 399-208 (2002)

8. Terrones M, Grobert N, Olivares J, Zhang J P, Terrones H, Kordatos K, Hsu W K, Hare J P, Townsend P D, Prassides K, Cheetham A K, Kroto H W and Walton D R M, "Controlled production of aligned-nanotube bundles," Nature 388, 52-5 (1997)

9. Seidel R, Duesberg G S, Unger E, Graham A P, Liebau M, Kreupl F, "Chemical Vapor Deposition Growth of Single-Walled Carbon Nanotubes at 600 °C and a Simple Growth Model," J Phys Chem B 108, 1888-1893 (2004)

10. Li W Z, Xie S S, Qian L X, Chang B H, Zou B S, Zhou W Y, Zhao R A, Want G, "Large-Scale Synthesis of Aligned Carbon Nanotubes," Science 274, 1701-1703 (1996)

11. Dong L, Jiao J, Pan C, Tuggle D W, "Effects of catalysts on the internal structures of carbon nanotubes and corresponding electron field-emission properties," Appl Phys A 78, 9-14 (2004)

12. Kumar A, Pushparaj V L, Kar S, Nalamasu O, Ajayan P M, "Contact transfer of aligned carbon nanotube arrays onto conducting substrates," Appl Phys Lett 89, 163120 (2006)

References

13. Huang S, Dai L, Mau A W H, "Patterned Growth and Contact Transfer of Well-Aligned Carbon Nanotube Films," J Phys Chem B 103, 4223-4227 (1999)
14. Yang J, Dai L, Vaia R A, "Multicomponent Interposed Carbon Nanotube Micropatterns by Region-Specific Contact Transfer and Self-Assembling," J Phys Chem B 107 12387-12390 (2003)
15. Chai Y, Gong J, Zhang K, Chan P C H, Yuen M M F, "Flexible transfer of aligned carbon nanotube films for integration at lower temperature," Nanotechnology 18 355709 (2007)
16. McCarter C M, Richards R F, Mesarovic S Dj, Richards C D, Bahr D F, McClain D, Jiao J, "Mechanical compliance of photolithographically defined vertically aligned carbon nanotube turf," J Mater Sci 41, 7872-7878 (2006)
17. French P J, "Polysilicon: a versatile material for Microsystems," Sens Act A 99, 3-12 (2002)
18. McClain D, Wu J F, Tavan N, Jiao J, McCarter C M, Richards R F, Mesarovic S, Richards C D, Bahr D F, "Electrostatic Shielding in Patterned Carbon Nanotube Field Emission Arrays," J Phys Chem C 111, 7514-7520 (2007)
19. Zbib A A, Mesarovic S Dj, Lilleodden E T, McClain D, Jiao J, Bahr D F, "The coordinated buckling of carbon nanotube turfs under uniform compression," Nanotechnology 19, 175704 (2008)

References

20. Kang N, Lu L, Kong W J, Hu J S, Yi W, Wang Y P, Zhang D L, Pan Z W, Xie S S, "Observation of a logarithmic temperature dependence of thermoelectric power in multiwall carbon nanotubes," Phys Rev B 67, 033404 (2003)
21. Wang D, Song P, Liu C, Wu W, Fan S, "Highly oriented carbon nanotube papers made of aligned carbon nanotubes," Nanotechnology 19, 075609 (2008)
22. Whitley E, Ball J, "Statistics review 6: Nonparametric methods," Crit Care 6 509-513 (2002)
23. Yaglioglu O, Hart A J, Martens R, Slocum, A H, "Method of characterizing electrical contact properties of carbon nanotube coated surfaces," Rev Sci Instrum 77, 095105 (2006)

Chapter Four

4. Mechanical Transfer in new configurations and electrical and thermal characterization of transferred VACNT turfs

4.1 Introduction

The previous chapter discussed details on the characterization of the mechanical transfer process for VACNT turfs. A model of separation was presented, with separation occurring in four discrete areas. First, any initial buckling in the turf is reversed. This is followed by an unwinding and detangling of the CNTs as the turf is extended. As the separation stress is reached, CNTs begin to separate from the sol-gel substrate. Finally, the final CNTs separate, and the transfer occurs.

An important observation in the previous chapter's results is the amount of deformation that a transferred VACNT turf can take without causing an appreciable change in resistance. The gold films encapsulating both sides of the VACNT serve as an electrical link between the nanotubes, allowing deformation to occur within the turf without having an appreciable impact on the electrical paths through the turf.

This chapter explores attempts at mechanical transfer for different configurations of VACNT turfs, including arrays of VACNT turfs, and trying to pull specifically patterned areas of a single large VACNT turf. Further electrical probing of both non-transferred gold coated VACNTs turfs and transferred VACNT turfs will be discussed, with a discussion on how the VACNT turfs behave electrically while being both heated and cooled and an exploration of the effect of turf size on electrical conductivity. The

chapter concludes with an overview of transfer of VACNTs onto Kapton and a comparison of mechanical and thermal values of VACNTs with published literature.

4.2 Mechanical transfer of VACNT arrays

All mechanical transfers of VACNTs described up to this point have been single VACNT turfs, with a size on the order of 4x4 mm^2. Arrays of VACNT turfs can be transferred in exactly the same method as was previous accomplished with the larger 4x4 mm^2 VACNT turfs. The amount of stress is applied in the same way, with the total contact area equaling the sum of the area of each individual VACNT turf. Thermocompression bonding occurs at 150 °C for a minimum of two hours. Array configurations vary from 20x20 to 60x60 individual VACNT turfs, with each turf varying from 20 to 60 μm in size.

Figure 4.1 shows the first successful transfer of an array of VACNT turfs. An observation of the results of the mechanical transfer of VACNT arrays brings into light new issues that must be taken into account. An immediate observation is the partial transfer of the arrays, including partial transfer of individual turfs, as shown in Figure 4.1.

(a) (b)

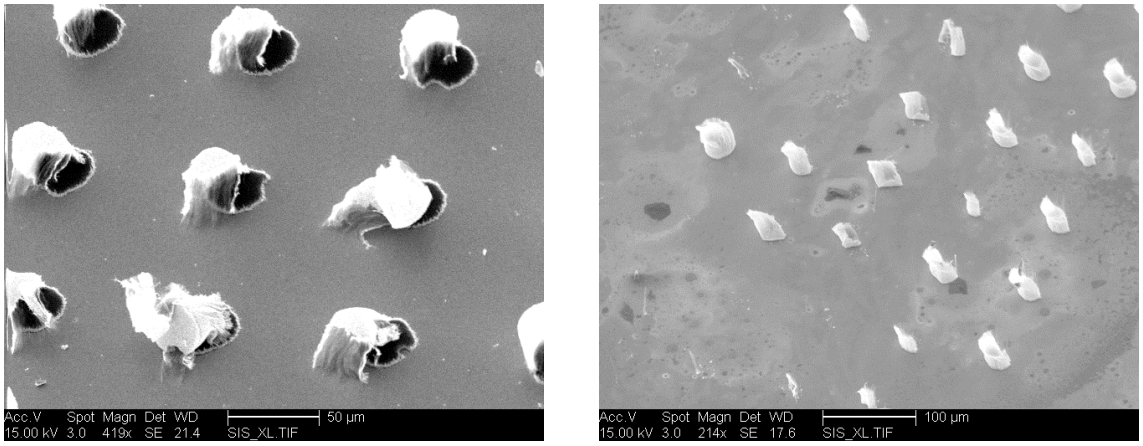

Figure 4.1 - (a) The original substrate after an attempt at mechanical transfer of an array of gold coated VACNT turfs (b) The transfer surface, showing partial transfer of the arrays

Another issue that requires care in the mechanical transfer of the VACNT turfs is verifying that the compression applied to the sandwich structure during thermocompression bonding is normal, minimizing any shear stress placed on the VACNT turf. In the case of a 4x4 mm^2 turf, it is able to resist more shear stress than smaller individual arrays, allowing for some leniency in the accuracy of the stress application to the sandwich structure. VACNT arrays are less resistant to shear forces, and will tend to collapse or fall over under the application of any shear stresses.

Clean mechanical transfer is further hindered by leaning of arrays, especially arrays with smaller areas. 4x4 mm^2 VACNT turfs do not lean, and the surface of the turf is parallel to the growth surface. This is not the case with arrays of VACNTs, as shown

in Figure 4.2, which shows part of an array of 20 μm VACNT turfs. This leaning makes mechanical transfer difficult, even when it is guaranteed that the applied load is perfectly normal with no shear loading.

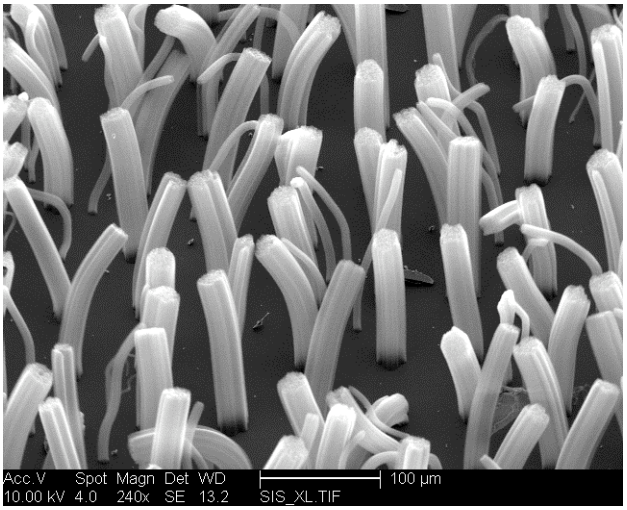

Figure 4.2 - SEM image of an array of uncoated VACNT turfs, demonstrating their tendency to lean during growth.

Another interesting observation of mechanical transfer of VACNT arrays occurs when the applied stress during mechanical transfer is beyond the buckling stress of the turf. The sputtering of the gold film on the VACNT turfs, while coating the top of the turf, will also coat the side of the VACNT turf. When the amount of stress applied is beyond the buckling stress, the turf collapses under the weight, pressing the gold coated sides of the turf against the growth substrate. These sides of the turf will bond with the growth substrate, and upon separation, the exterior of the turf will remain on the substrate, while the interior, which doesn't have a side in contact with the growth

substrate, will transfer. Figure 4.3 shows both the growth substrate and the transfer substrate, as well as a diagram showing what is taking place.

(a) (b)

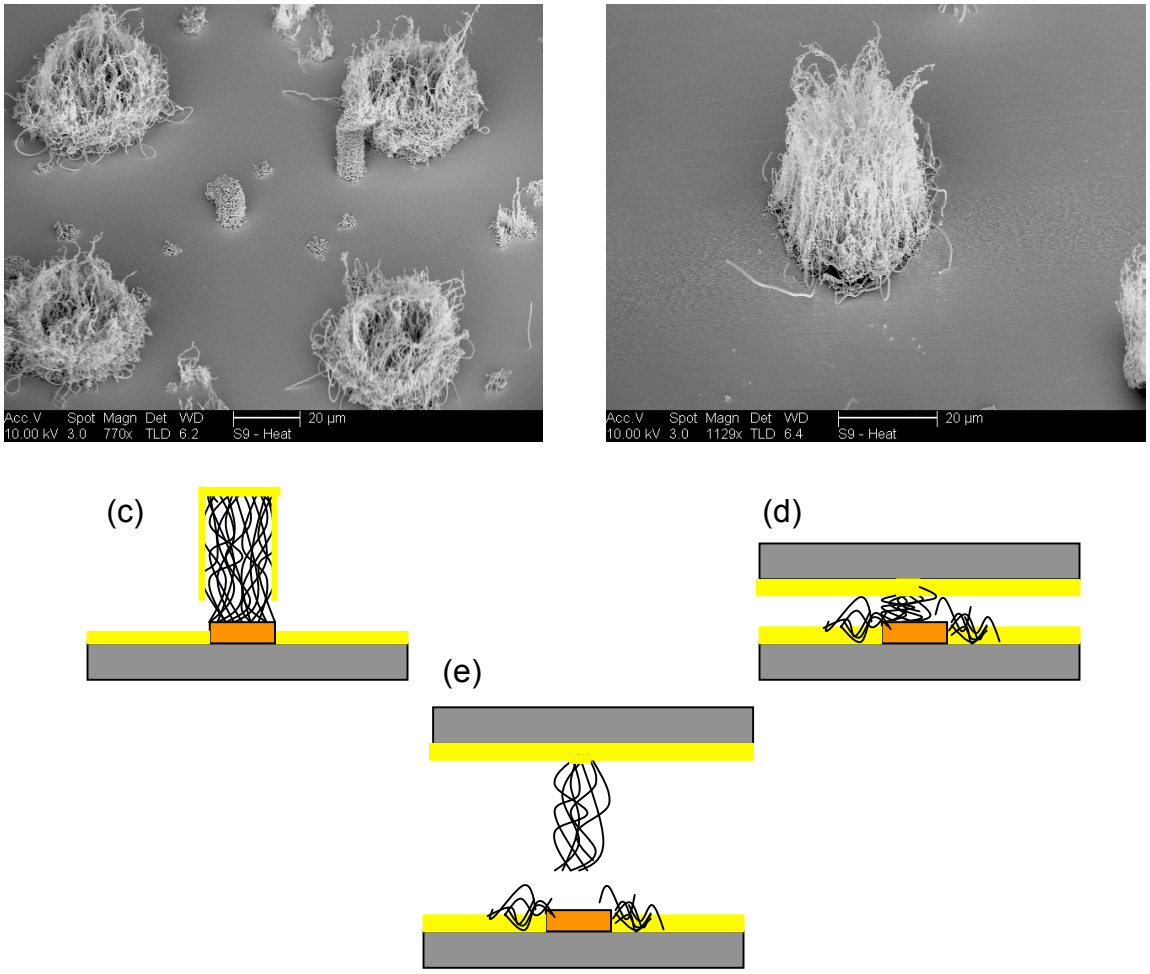

Figure 4.3 - (a) The remains of VACNT turfs left behind as a result of heavy deformation due to excessive buckling (b) The interior of a VACNT array, transferred to the new substrate (c) (d) (e) A diagram modeling deformation

4.3 Patterned mechanical transfer

Low-temperature mechanical transfer of VACNT turfs at 150 °C has been demonstrated and characterized in the previous chapters. The process pulls entire pre-patterned VACNT turfs in their entirety to the new substrate. A logical next step would be to attempt to transfer specific areas of one complete turf.

A 4x4 mm^2 VACNT turf is coated in 5 nm of TiW, followed by 300 nm of gold. The steps for patterning the silicon wafer that the VACNT turf will be patterned to is detailed in Figure 4.4. The silicon contacting surface (a) that the VACNT turf will be transferred to first has a 150 nm thermal oxide film grown (b). A 5 nm adhesion layer and a 300 nm gold film are deposited (c). An HDMS binder layer and a layer of AZ 5214 photoresist are each spun on the wafer at 3000 rpm for 30 seconds (d). The photolithography mask is placed over the top of the silicon wafer, and then the photoresist not concealed by the mask is exposed to UV light for 12 seconds (e). The wafer is placed in a 4:1 ratio AZ 400K developer:DI water solution to wash away exposed photoresist, leaving photoresist on areas where gold is to remain (f). The wafer is then placed in a gold etch solution, which etches away any part of the gold film that is not covered by the photoresist (g). Upon removal of remaining photoresist using acetone, patterned gold features remain on the silicon wafer (h).

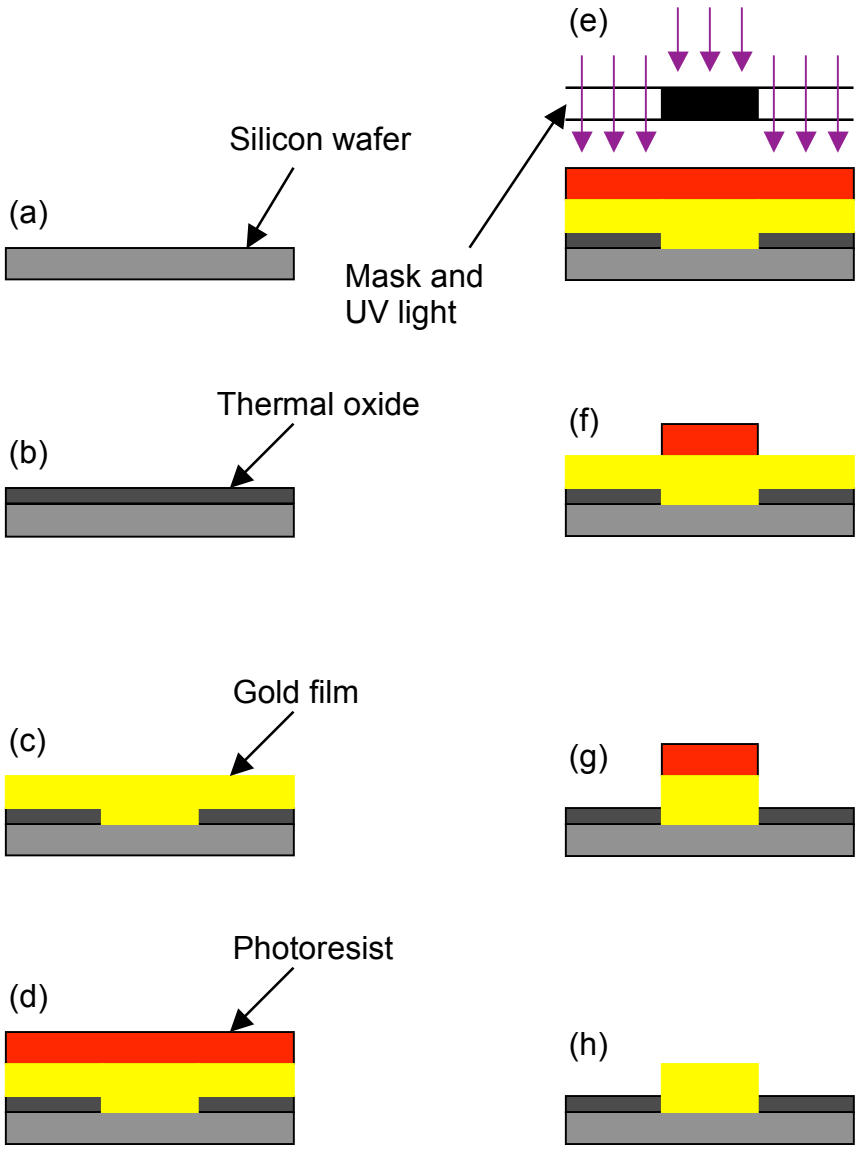

Figure 4.4 - Process of patterning gold for patterned mechanical transfer of VACNT turfs.

The mechanical transfer occurs as before, with the patterned gold wafer being brought into contact with a VACNT turf, coated with a 5 nm TiW adhesion layer and 300 nm of gold. The structure is compressed according to the buckling stress of the turf, and heated to 150 °C for a minimum of two hours. As shown previously, gold coated VACNT turfs will not bond to an uncoated silicon wafer, and due to the inertness of the silicon oxide film, will not bond to the silicon oxide film either. Upon separation of the structure, any part of the VACNT turf in contact with the patterned gold on the silicon wafer will transfer, leaving any part of the VACNT turf not in contact with the patterned gold on its original substrate. This method provides an alternative method of mechanical transfer of patterned VACNT arrays by allowing the arrays to be patterned out of one large VACNT turf, rather than growing the patterned arrays during CVD and mechanically transferring all of the turfs in their entirety. This process is detailed in Figure 4.5, with an SEM image of a part of the resulting transfer shown in Figure 4.6. Figure 4.7 shows the original VACNT substrate where the patterned transfer occurred, showing a hole in the VACNT substrate that VACNTs were pulled from.

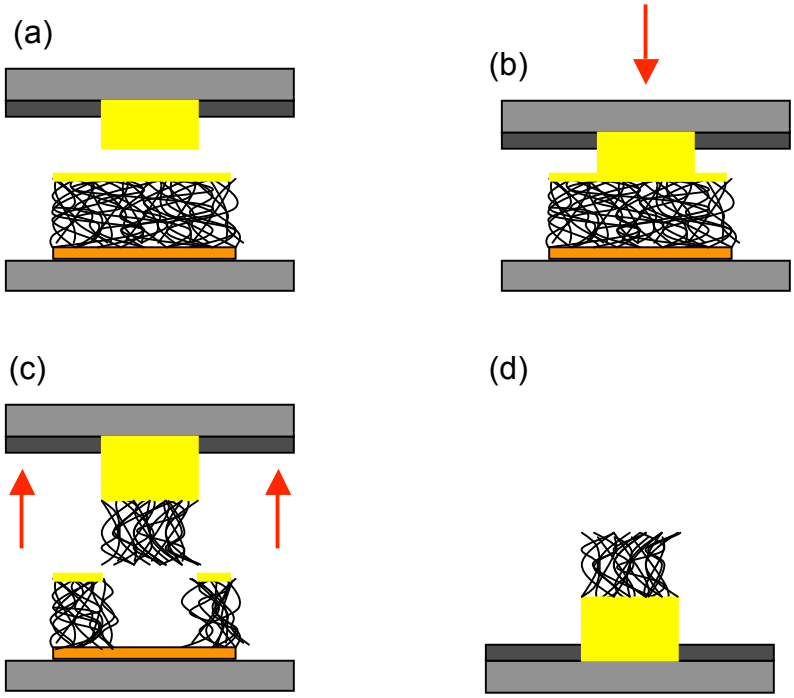

Figure 4.5 - A diagram showing patterned mechanical transfer of a VACNT turf.

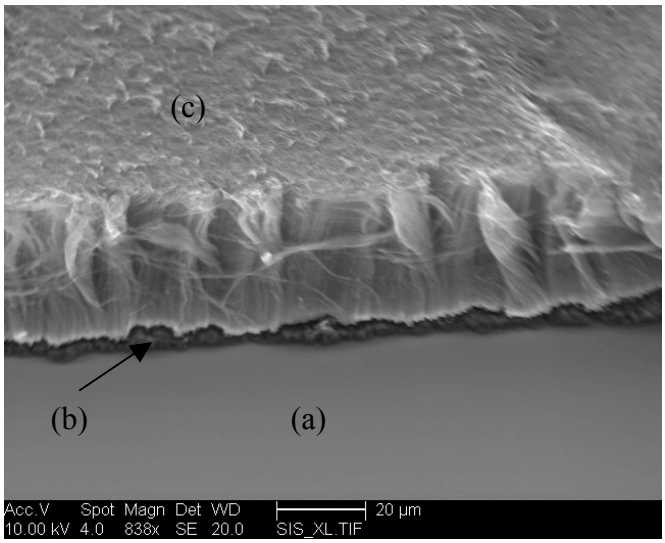

Figure 4.6 - An SEM image of a patterned, mechanically transferred VACNT turf. (a) silicon oxide (b) Start of patterned gold area (c) transferred VACNT turf, pulled off of larger VACNT turf.

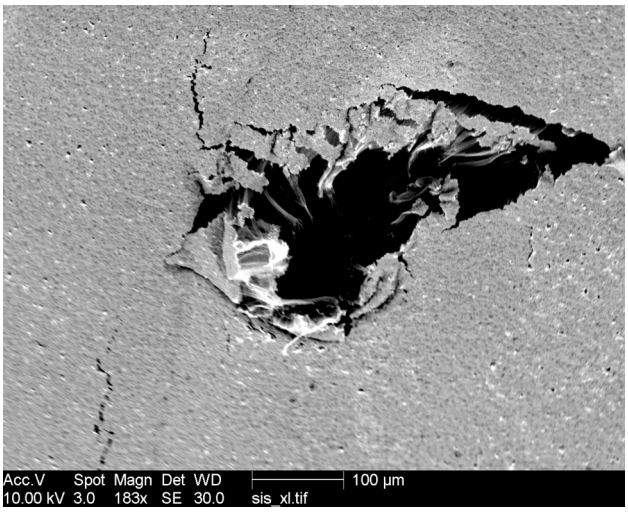

Figure 4.7 - Hole in original VACNT turf as a result of patterned transfer.

4.4 Thermal Annealing of VACNT turfs

The mechanical transfer process has the important effect of removing the VACNT turf from its sol-gel substrate, thus removing an insulating layer and improving electrical and thermal conductivity. It is desirable to understand the effects of thermal annealing of the gold film after mechanical transfer on the electrical conductivity of the VACNT turf with the goal of seeing further improvement in electrical conductivity.

Transferred VACNT turfs with 5 nm TiW and 300 nm of gold sputtered on the top of the transferred VACNT turf first had electrical leads bonded to them using conductive epoxy, in order to provide an electrical bypass from the silicon wafer. A tungsten-carbide probe tip was brought into contact with the top of the gold coated VACNT turf, with care being taken to avoid deformation of the turf. The gold coating prevents adhesion between the VACNT turf and the tungsten-carbide probe, allowing

repeated contacts to be made without damaging the turf or having bonded CNTs cause issues with subsequent resistance measurements.

Initial measurements across nine VACNT turfs showed an electrical resistance of approximately 20 Ω. The samples were then annealed at 250 °C for two hours. Electrical resistance measurements were taken again, showing an average of approximately 10 Ω, showing an improvement of ~10 Ω. It is necessary to back out where this improvement is occurring. Three areas of potential improvement are assumed, with a further assumption that the low temperatures have no effect on the conductivity of the CNTs with the turf. Areas of improvement are the Au/Au interface, the gold film in the path to the conductive epoxy, and the conductive epoxy itself.

One more sample with transferred, gold coated VACNT arrays had electrical leads attached. Two blank gold coated silicon wafers had electrical leads attached to them, with the intention of analyzing the change in electrical resistance in the conductive epoxy due to the annealing. The electrical resistance of the samples with just the epoxy were measured to be 7.2 Ω and 3.4 Ω respectively. After two hours of annealing at 250 °C, the resistance dropped to 1.5 Ω in both samples. This demonstrates a change in electrical resistance in the epoxy due to annealing.

The sample with arrays had the tungsten-carbide probe carefully dropped on the VACNT turfs, and produced electrical resistance measurements ranging from 5.2 Ω to 5.9 Ω. The probe was also directly dropped on the gold film, and measured a resistance of 6.4 Ω. Upon annealing, turf measurement ranged from 3.1 Ω to 3.8 Ω, with a film resistance of 2.2 Ω.

The results make it difficult to conclude an effect of annealing at 250 °C on the Au/Au interface. Further data will have to be collected to make a reasonable conclusion.

4.5 Electrical resistance measurements vs temperature

Experiments were conducted to measure electrical resistance vs temperature of a gold coated transferred VACNT turf, with the purpose of seeing how much the resistance of the structure changes within a potential operating temperature range for a device. With the previous tests, each individual electrical resistance measurement was taken by bring the tungsten-carbide probe up and then back down onto a turf. Although there is no issue with CNTs attaching themselves to the probe, due to the gold coating on the VACNT turf, there is still an issue due to the morphology of the turf. The top of VACNT turfs have a random structure, meaning that each contact on a different part of a turf will contact in a different way with a different contact area. This produces noise in electrical resistance measurements. To eliminate uncontrollable differences between repeated contacts, a single contact was made, and the temperature was changed with contact maintained. Electrical resistance effects due to both heating and cooling were measured.

A transferred, gold coated VACNT turf was placed on a hotplate, and a probe was brought into contact. Temperature was swept from 0 °C to 250 °C. Resistance measurements are shown in Figure 4.8. The structures displayed an increase on the order of 1 Ω as the temperature increased.

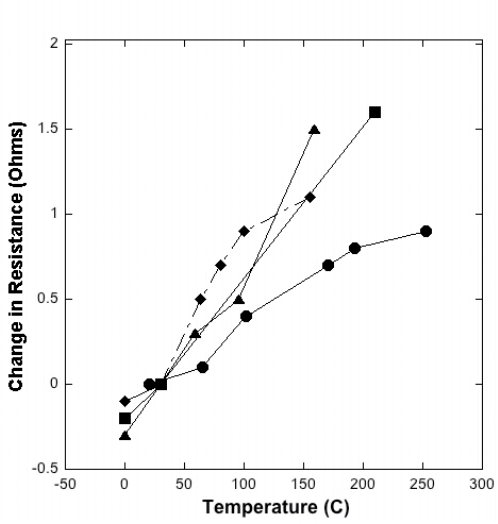

Figure 4.8 - Change in resistance vs temperature for a gold coated VACNT turf with room temperature as a reference temperature

4.6 Mechanical Transfer onto Kapton

Flexible electronics have been a subject of intense research, producing applications as varied as organic transistors[1], or flexible electrodes for analyzing brain signals in rats.[2] It is desirable to apply the mechanical transfer method to determine if VACNTs can be transferred to flexible substrates.

A 25 μm flexible Kapton film, coating with 5 nm TiW layer and 300 nm of gold, is brought into contact with a similarly coated VACNT turf. The same mechanical transfer process is used, with pressure applied according to the buckling model, for a minimum of two hours at 150 °C. Upon separation, the VACNT turf transferred to the flexible Kapton substrate, as shown in Figure 4.9 This process can be applied towards new applications for CNTs in flexible electronics.

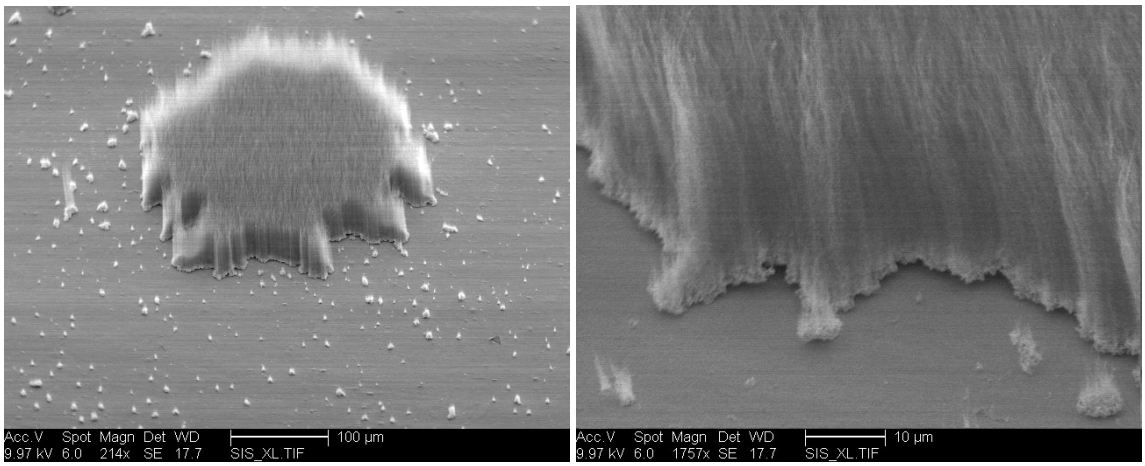

Figure 4.9 - VACNT turf transferred onto a flexible Kapton substrate.

4.7 Mechanical and Thermal Properties Compared with Literature

A comparison of separation stress and thermal resistance values for VACNT turfs is provided in Table 4.1. Bonding strength through the strength of the Au/Au interface is compared to the separation strength of CNTs bonded to glass as shown by Fisher. Thermal resistance measurements of the VACNT turfs are provided by Cho, and are compared to measurements of VACNT thermal interfaces constructed by Fisher under ~1 N loading. Fisher's values are stated in mm^2 * K / W, while Cho's are stated in °C / K. By multiplying Cho's value by the lateral area of the VACNT turfs measured, which in this case was 16 mm^2, the areas are normalized.

	Thermal resistance (mm^2 * K / W)
Cho - non-transffered VACNT turf	160
Cho - Au coated non-transffered VACNT turf	560
Cho - Au coated transferred VACNT turf	320
Cho - transferred bonded VACNT thermal interface	100
Fisher - VACNT thermal interface	19.8

	Interface Strength (Mpa)
Au/Au Interface	0.553
Fisher - VACNTs on glass	0.044

Table 4.1 - Comparisons of thermal and mechanical properties of VACNT turfs with published literature.[3,4,5]

The Au/Au interface demonstrates a strength a factor of 10 greater than the strength of the VACNTs on glass, which was bonded using anodic bonding. Fisher's measurement of the thermal interface was not conducted using the VACNTs on glass, so it is difficult to correlate differences in bonding strength with differences in thermal resistance. In Fisher's thermal measurements, the thermal resistance of only the VACNTs was calculated, whereas in Cho's measurements, the entire devices thermal resistance was measured. Cho's device is larger overall, which leads to part of the

increase in thermal resistance. Overall, the Au/Au bonded structure has a higher thermal resistance than what is measured by Fisher. However, with the transferred VACNTs being on a conductive substrate, they are still applicable as a thermal switch or a thermal interface material.

4.8 Conclusion

This chapter demonstrated the application of the new mechanical transfer process in a couple of different configurations, including transferring arrays of VACNTs rather than a single large VACNT, and pulling patterned areas off of a large VACNT. Although there are issues to overcome before clean mechanical transfer can be accomplished using this process, some flexibility in the process is demonstrated.

Initial experiments in thermal annealing and electrical resistance measurements during heating and cooling were discussed. Thermal annealing has been shown to have little overall effect on improving electrical resistance. Electrical measurements during heating demonstrate that gold coated VACNT turfs demonstrate an increase of approximately 1 Ω when temperature is swept up to 250 °C. Finally, mechanical and thermal properties of the VACNT turfs were compared with literature.

References

[1] Crone B, Dodabalapur A, Lin Y Y, Filas R W, Bao Z, LaDuca A, Sarpeshkar R, Katz H E, Li W, "Large-scale complementary integrated circuits based on organic transistors," Nature 403, 521 (2000)

References

[2] Yeager J D, Phillips D J, Rector D M, Bahr D F, "Characterization of flexible ECoG electrode arrays for chronic recording in awake rats," J Neurosci Meth 173, 279 (2008)

[3] Aradhya S V, Garimella S V, Fisher T S, "Electrothermal Bonding of Carbon Nanotubes to Glass," J Electrochem Soc 155, K161 (2008)

[4] Cho J H, "Design, Fabrication, and Characterization of a MEMS Thermal Switch and Integration with a Dynamic Micro Heat Engine," [PhD Dissertation]: Washington State University (2007)

[5] Xu J, Fisher T S, "Enhanced Thermal Contact Conductance Using Carbon Nanotube Array Interfaces," IEEE T Compon Pack T 29, 261 (2006)

CHAPTER FIVE

5. CONCLUSION AND RECOMMENDATION FOR FUTURE WORK

A new procedure for the integration of VACNT turfs into MEMS devices has been developed, which allows for the direct transfer of VACNT turfs through low-temperature thermocompression bonding. This method shows promise as a technique to allow for the integration of VACNTs in MEMS and microelectronics applications. Application of the same technique has been successful for similar VACNT configurations, including transferring arrays of VACNT turfs, or pulling patterned areas off of a large VACNT turf.

The average separation stress off of the sol-gel substrate is 0.42 MPa, while the average separation stress of the Au/Au interface is 0.553 MPa. Electrical measurements during mechanical transfer of a VACNT turf with Au films on either side demonstrates little change in electrical resistance, even with a considerable amount of deformation in excess of 200%. This is believed to be a result of the gold film on either side of the turf providing an electrical link between the individual CNTs, placing less dependence on the linking of CNTs within the VACNT turf structure. When the VACNT turf is compressed, its nominal density increases, and the amount of entanglement logically increases. Conversely, as a turf is extended, the nominal density decreases, and the amount of entanglement decreases. In both cases, the electrical resistance of a gold coated VACNT turf changes very little, suggesting that linking between the CNTs within the turf has little effect on the overall electrical conductivity.

This research shows a lot of promise for future projects. Further analysis of the effects of CNT entanglement needs to be done. By measuring the lateral resistance across the VACNT turf during sandwich structure separation, analysis of electrical resistance due to entanglement can be analyzed. An understanding of the CNT entanglement's effect on electrical and thermal conductivity is important to fully understand how conductivity is affected by entanglement of CNTs.

An important experiment in the attempts to apply VACNTs to MEMS and microelectronics is an understanding of the elastic properties of the VACNT turf. This can be done by stepping up and holding the load as the VACNT turf is being separated and measuring the electrical resistance.

Although contact area is increased as a result of the gold film, the packing fraction of VACNT turfs is low, and can still be increased. Processing methods can be explored to grow denser turfs. The strength of the Au/Au bond needs to be explored in greater depth, including finding methods to increase the strength of the bond.

Mechanical transfer in this thesis was accomplished using thermal heating in a furnace. A potential alternative to thermal heating that can be explored is joule heating through the application of current as the gold film on top of the VACNT turf and the gold film on the silicon wafer are compressed together. To reduce the 2 hour bonding time, which is still very high, supersonic bonding can be explored, which is a common process in wire bonding in semiconductor processing. It is unknown what effect supersonic bonding will have on the structure of the VACNT turf.

Long-term effects of the usage of transferred VACNTs in MEMS and microelectronics applications needs to be explored. The long-term effects of mechanical

and thermal cycling, thermal expansion effects within the VACNT turf, and potential oxidation are all effects that need to be explored further.